JOURNAL OF GEOPHYSICAL RESEARCH, VOL. 112, C05010, doi:10.1029/2006JC003891, 2007

Uncertainties in the mean ocean dynamic topography before the launch of the Gravity Field and Steady-State Ocean Circulation Explorer (GOCE)

Femke C. Vossepoel[1,2]

Received 18 August 2006; revised 15 November 2006; accepted 29 November 2006; published 4 May 2007.

[1] In anticipation of the future observations of the gravity mission Gravity Field and Steady-State Ocean Circulation Explorer (GOCE), the present-day accuracy of mean dynamic topography (MDT) is estimated from both observations and models. A comparison of five observational estimates illustrates that RMS differences in MDT vary from 4.2 to 10.5 cm after low-pass filtering the fields with a Hamming window with wavenumber $N = 120$ (corresponding to an effective resolution of 167 km). RMS differences in observational MDT reduce to 2.4–8.3 cm for $N = 15$ (1334 km). Differences in data sources (geoid model, in situ data) are mostly visible in the small-scale oceanic features, while differences in processing (filtering, inverse modeling techniques) are reflected at larger scales. A comparison of seven different numerical ocean models demonstrates that model estimates differ mostly in western boundary currents and in the Antarctic Circumpolar Current. RMS differences between modeled and observed MDT are at best 8.8 cm for $N = 120$, and reduce to 6.4 cm for $N = 15$. For models with data assimilation, a minimal RMS difference of 6.6 cm ($N = 120$) to 3.4 cm ($N = 15$) is obtained with respect to the observational MDTs. The reduction of differences between MDTs with increasing filtering scales is smaller than expected. While it is expected that GOCE will improve MDT estimates at small spatial scales, improvement of mean sea surface estimates from satellite altimetry may be needed to improve MDT estimates at larger scales.

Citation: Vossepoel, F. C. (2007), Uncertainties in the mean ocean dynamic topography before the launch of the Gravity Field and Steady-State Ocean Circulation Explorer (GOCE), *J. Geophys. Res.*, *112*, C05010, doi:10.1029/2006JC003891.

1. Introduction

[2] The dynamic topography is the distance between the ocean surface and the gravity equipotential surface called the geoid. As it reflects the geostrophic currents at the surface, it is of great interest for ocean circulation studies. The time-mean dynamic topography (MDT) is the average of the dynamic topography over a particular time period. Assuming that this time period is long enough for the ocean to reach a steady state, the MDT can be interpreted as the steady state component of the ocean circulation. Originally, methods of estimating MDT were based entirely on hydrographic data assuming a level of no motion [*Sverdrup et al.*, 1942]. This approach was replaced by mass conservation, either through inverse methods [*Wunsch*, 1978], or through other methodologies [e.g., *Reid*, 1997].

[3] Inverse models allow a combination of different data types, including satellite data [*Wunsch*, 1996]. For example, MDTs have been derived from a combination of satellite altimetry and subsurface drifters [*Maximenko and Niiler*, 2004; *Rio and Hernandez*, 2004]. Altimeter-based MDT estimates require at least two data sets: the mean sea surface height relative to an ellipsoid from satellite altimetry (MSS, again, averaged over a time period long enough to reach a steady state) [*Hernandez et al.*, 2001; *Wang*, 2001] and the geoid height relative to the same ellipsoid. Originally, geoid models were based on terrestrial measurements and/or satellite orbit analysis, but recent geoid estimates include data from dedicated gravitational missions such as CHAMP (CHAllenging Minisatellite Payload) and GRACE (Gravity Recovery and Climate Experiment) [*Reigber et al.*, 2005; *Tapley et al.*, 2003]. Time variations in the geoid are much smaller than in the MSS and consequently their effect on the mean geoid estimate will be negligibly small. However, the GRACE geoid error spectrum decreases with increasing wavelength and time-averaging many months or even several years of GRACE data is necessary to reduce these errors. The need for time-averaging is less strong when using GOCE data, as this satellite is more sensitive to short-wavelength geoid signals resulting in a more accurate geoid at short length scales when averaging over a relatively short period.

[4] After pioneering studies with the Seasat altimeter observations [e.g., *Cheney and Marsh*, 1981; *Zlotnicki*, 1984; *Engelis and Knudsen*, 1989], the longer time series

[1] Institute of Marine and Atmospheric Research Utrecht (IMAU) and SRON Netherlands Institute for Space Research, Utrecht, Netherlands.
[2] Now at Shell International Exploration and Production B.V., Rijswijk, Netherlands.

0148-0227/07/2006JC003891$09.00

of the Geosat altimeter allowed a reasonable estimation of a satellite-derived global mean dynamic topography [e.g., *Nerem et al.*, 1990; *Denker and Rapp*, 1990]. At that time, the geoid error at scales smaller than 4000 km was too large to allow for high-resolution MDT estimates. In addition, MDT accuracy was strongly affected by orbit errors as well as errors in the observational corrections, such as the correction for the effect of surface waves, tides, and atmospheric pressure on sea surface height. With the TOPEX/Poseidon mission more precise estimates of the mean dynamic topography could be obtained [*Rapp et al.*, 1996; *Stammer*, 1994] as orbit and geoid accuracy had improved and errors in observational corrections had been reduced. However, then still, the geoid errors were very much limiting the accuracy of the MDT estimates. Only recently, the GRACE mission has contributed to a considerable reduction in geoid error [*Tapley et al.*, 2003]. In fact, the accuracy of a GRACE-based geoid for MDT estimation is significantly higher than previous geoid estimates, as shown by a regional comparison of MDTs in the North Atlantic [*Jayne*, 2006].

[5] Over the last few decades, technological developments as well as increased computational resources stimulated the development of more realistic Ocean General Circulation Models (OGCMs) (for an overview, see for example *Willebrand et al.* [2001], *Griffies et al.* [2000], and *Griffies* [2005]). The time-average of model sea surface height is itself a mean dynamic topography, which reflects the steady state component of the circulation as simulated by the model.

[6] OGCMs are generally categorized in terms of their vertical discretization. The most straightforward choice for vertical coordinates is on the basis of depth. These depth-level (or z-level) coordinates were applied in the first OGCMs [*Bryan*, 1969; *Semtner*, 1974; *Cox*, 1984]. Using the fact that most of the ocean circulation takes place along lines of constant density, so-called isopycnal coordinates were introduced that provide a natural discretization of the water column [e.g., *Bleck*, 1998]. While the z-level coordinate is especially useful in weakly stratified regions such as the mixed layer, the isopycnal coordinates provide a more efficient discretization of the ocean at depth. A third class of OGCMs, based on terrain-following (or sigma) coordinates is especially useful in coastal regions [*Blumberg and Mellor*, 1987]. Hybrid models, such as the Hybrid Coordinate Ocean Model combine the advantages of these different discretizations, adapting the discretization for regions with different dynamical characteristics [*Chassignet et al.*, 2006]. In addition to the direct impact of vertical discretization on sea level, the difference in vertical discretization also implies a difference in the representation of the bathymetry, which causes an additional effect on modeled MDT.

[7] From the original z-level models, which were based on the rigid-lid assumption that eliminates high-speed external gravity waves and allows a longer time step, sea level height could be derived a posteriori applying thermal wind equations. The development of free-surface formulations [e.g., *Dukowicz and Smith*, 1994; *Roullet and Madec*, 2000], allowed a direct computation of sea level height in z-level models. In isopycnal and sigma-coordinate models, the computation of sea level follows from the thickness of the layers.

[8] While first OGCMs had a horizontal resolution of 2, current OGCMs are configured at eddy-resolving resolution of one tenth to One twelfth of a degree [*Maltrud and McClean*, 2005; *Chassignet et al.*, 2006], leading to a highly accurate representation of oceanic fronts and meanders in model sea level height. In addition to the improvements in resolution, discretization and representation of bathymetry, refinement in sub-grid-scale mixing parameterizations [*Cox*, 1997; *Gent and McWilliams*, 1990; *Large et al.*, 1994] and the availability of long time series of global analyses of atmospheric forcing fields from models and (satellite) data [e.g., *Kalnay et al.*, 1996; *Gibson et al.*, 1997] further increased the accuracy of modeled ocean circulation and associated MDT.

[9] On one hand, the increasing accuracy of both observed and modeled MDTs allows altimetric data to be combined with a geoid model into ocean general circulation models [*Stammer et al.*, 2002], and to assess the impact of assimilated dynamic topography on the simulation of ocean currents [*Birol et al.*, 2004, 2005]. On the other hand, it enables investigations to the effect of geoid error on transport estimates when combining altimetry with hydrographic sections in inverse estimates [*LeGrand*, 2001; *Schröter et al.*, 2002; *Losch and Schröter*, 2004]. Using a combination of models assimilating observations, *Bingham and Haines* [2006] demonstrated that it is now possible to generate a regional MDT as accurate as 3.2 cm RMS at a spatial resolution of 1°.

[10] On the verge of the launch of the Gravity and Ocean Circulation Explorer (GOCE), which promises to further reduce geoid errors at spatial scales of about 100 km [*European Space Agency*, 1999], this study examines the present-day uncertainties in MDT estimates from observations and state-of-the-art ocean numerical models. The objective of this study is to evaluate recent estimates of MDT, to quantify their mutual differences, and to identify the regions of largest uncertainties in these estimates.

[11] The outline of this paper is as follows. In section 2, five different observational estimates of the dynamic topography are presented and compared. Mean dynamic topography estimates from numerical models are described and compared in section 3. Section 4 describes a comparison of the model solutions with one of the observational dynamic topography estimates. Section 5 concludes with a summary and discussion.

2. Observational Estimates of the Mean Dynamic Topography

[12] When subtracting a geoid model from the altimeter based MSS to obtain an MDT, a number of issues need to be considered. Foremost, the geoid has about 2 orders of magnitude more energy than the MDT at all wavelengths [*Wagner and Colombo*, 1979], which implies that MSSs derived from altimetry are dominated by geoid information. This is not only the case at the very long wavelengths, but also down to wavelengths of a few tens of kilometers. However, satellite derived, global geoids are accurate up to wavelengths of hundreds of kilometers only [*Tapley et al.*, 2003] and have no information about the gravity field at wavelengths much shorter than the satellite altitude. As a consequence, the shorter wavelength geoid information

Table 1. Overview of Observation-Derived Dynamic Topographies[a]

MDT	Observations	Geoid (Degree/Order)	Resolution
Rio05	MSS-CLS01 (TOPEX/Poseidon, ERS-1,2, Geosat), GRACE,CHAMP and in situ oceanographic obs	EIGEN-3 (30)	0.5°
Chambers-Zlotnicki	GSFC MSS 00 (TOPEX/Poseidon, ERS-1,2, Geosat), GRACE and surface gravity obs	GGM02c (360)	0.5°
Naeije	MSS-CLS01 (TOPEX/Poseidon, ERS-1,2, Geosat), GRACE and surface gravity obs	GGM02c (360)	0.5°
LeGrande	*Gouretski and Jancke* [2001] climatology, 5-year T/P	EGM96 (180)	1.0°
Maximenko-Niiler	10-year drifter data set [*Niiler*, 2001], JPL mean sea level using GRACE GGM01, NCAR/NCEP re-analysis winds	GGM01 (90)	0.5°

[a]The resolution indicated is the resolution on which the grids are provided. The effective resolution may be different as a result of the processing.

which is present in the MSS but not in the geoid estimate, should be removed, minimizing leakage of small-scale geoid error into longer wavelengths of the geoid estimate. Furthermore, the satellite geoid is global but the MSS only exists over the oceans. The above issues make the computation of an observational MDT a challenging and delicate task. The various estimates of MDT from MSS and geoid model took different approaches to solve this problem [see *Rio and Hernandez*, 2004; *Chambers and Zlotnicki*, 2004; *Jayne*, 2006].

[13] In this study, five different observational estimates of the global MDT have been analyzed. They are summarized in Table 1. All estimates include satellite altimeter data, but the additional data sets vary as well as the filtering and the geoid models used. A further description of the processing methodology is given below.

2.1. LeGrand

[14] *LeGrand et al.* [2003] have based their dynamic ocean topography on 5 years of TOPEX/Poseidon data (1993–1997), combined with an estimate of dynamic ocean topography from D. P. Chambers of the Center for Space Research, University of Texas at Austin, relative to the EGM96 geoid [*Lemoine et al.*, 1998]. In addition, a gridded historical climatological data set derived from in situ observation by *Gouretski and Jancke* [2001] has been included in the estimate. The topography has been computed with a finite difference inverse model of the ocean circulation developed at the Laboratoire des Physique des Océans in Brest [*Mercier et al.*, 1993; *LeGrand et al.*, 1998]. The MDT is computed on a grid with a 1° spatial resolution.

2.2. Naeije

[15] The Naeije MDT (M.C. Naeije, personal communication, 2006) has been constructed at the Department of Earth Observation and Space Systems Research (DEOS) in Delft by subtracting GGM02c geoid [*Tapley et al.*, 2003] from the CLS01 MSS [*Hernandez et al.*, 2001] based on altimetric data of different satellite missions (Geosat, ERS1-2, and TOPEX/Poseidon) over the period 1993–1999. Because of the differences in spatial resolution of the geoid and the MSS and large gradients that may occur in the MSS, special attention has been paid to the way in which the two fields have been subtracted. For each location on a 0.5° grid the point value of the geoid height has been determined without interpolation or averaging. The corresponding MSS point values have been determined at exactly the same locations, again without interpolation or averaging. The resulting difference field has been smoothed with a Gaussian filter using a 1-sigma value of 1.5°, removing variations in the MDT with scales smaller than 300 km. Both MSS and geoid model were determined in the mean-tide reference frame. At the grid points over land the MDT has been set to the EGM96 geoid. The Naeije MDT grid is provided at a 0.5° resolution.

2.3. Chambers-Zlotnicki

[16] The Chambers-Zlotnicki MDT [*Chambers and Zlotnicki*, 2004] is based on the mean sea surface from Goddard Space Flight Center: GSFC MS 00 [*Wang*, 2001]. This estimate includes data from TOPEX/Poseidon, ERS-1 and -2 and Geosat, and is representative for the mean sea surface of the 1990s. From this mean sea surface, the GGM02c geoid has been deducted. This geoid is based on 363 days of GRACE data, spanning April 2002 and December 2003, complemented with surface gravity data to degree and order 360. The data have been filtered to remove the energy in the gravity field at wavelengths shorter than 400 km, as these can not be recovered by the GRACE satellites. The details of the processing can be found on the GRACE website (http://gracetellus.jpl.nasa.gov/dot.html) and in the paper by *Tapley et al.* [2003], which describes the generation of an earlier version of the MDT.

2.4. Rio05

[17] The Collecte, Localisation, Satellites (CLS) combined mean dynamic topography Rio05 [*Rio et al.*, 2005] is computed using a two-step procedure. In the first step, a large-scale estimate of the MDT is obtained subtracting the EIGEN-GRACE3S geoid model from the CLS01 MSS, both fields having been preliminary filtered from scales shorter than 400 km using a Gaussian low-pass filter. Note that the CLS01 MSS is the same that has been used for the Naeije MDT. The EIGEN-GRACE-03S geoid includes 376 days of GRACE data and is computed similarly to the EIGEN-GRACE02S geoid as described by *Reigber et al.* [2005]. It does not include any terrestrial gravity observations. At latitudes equatorward of 40° data from the Levitus climatology relative to 1500 m depth is also included. In the second step, the altimeter sea level anomalies are used to remove the time-dependent signal from the in situ measurements resulting in a synthetic estimate of the MDT. The in situ data used are surface drifter velocities from the World Ocean Circulation Experiment (WOCE) and Tropical Ocean and Global Atmosphere (TOGA) Surface Velocity Program (SVP) plus additional hydrographic profiles to a depth of 1500 meters from the French Coriolis data center for the period 1993–

2002. To achieve consistency with the altimetric content, further processing is applied to the in situ data sets. To obtain the geostrophic component of the surface velocity, Ekman surface currents are modeled and subtracted from the drifting buoy velocity data followed by removing high-frequency signals with a 3-day low-pass filter. A remove-restore procedure is then applied in which the obtained synthetic estimate of the MDT is used to improve the first guess through a multivariate objective analysis. More details of the processing are given by *Rio and Hernandez* [2004], who describe an earlier version of the topography. By choosing a reference depth of 1500 m, the dynamic topography signal below this level is not included in the hydrography. To correct for this, the signal is estimated subtracting the 1500 m Levitus climatology from the 400 km resolution GRACE MDT. This estimate of the 1500 m signal is then added to the dynamic heights relative to 1500 m to recover the dynamic topography signal over the whole water column (M.-H. Rio, personal communication, 2006). Therefore the synthetic estimate of the MDT represents the full oceanographic signal and so does the resulting topography. Note that the MDT is displaced vertically to match the dynamic topography between 40°N and 40°S computed from the *Levitus et al.* [1998] climatology. This causes the MDT to be offset with respect to other MDT estimates.

2.5. Maximenko-Niiler

[18] *Maximenko and Niiler* [2004] have used a simplified form of the horizontal momentum equation at 15 m depth to estimate a 10-year mean tilt of the absolute dynamic topography. The equation describes the balance of four terms: acceleration, Coriolis force, pressure gradient and vertical friction. In development of their previous technique [*Niiler et al.*, 2003], they estimated the terms in this equation not only with the aid of surface drifters [*Niiler*, 2001], Aviso sea level anomaly and wind fields from the National Centers for Environmental Prediction (NCEP), but also utilized an MDT generated at the NASA Jet Propulsion Laboratory by V. Zlotnicki, one of the early MDTs based on the first year of data from the GRACE mission. This altimeter-based MDT has been generated with the NASA GSFC MSS 00 of *Wang* [2001] (see description at Chambers-Zlotnicki MDT), truncated at degree and order 360, and subsampled to 0.5°. The MSS has been referenced to a GRACE-based geoid one version earlier than GGM01 [*Tapley et al.*, 2003], truncated at degree and order 90. The differences have been smoothed with a two-pass spatial averaging filter of approximately 1000 km (V. Zlotnicki, personal communication, 2006). Maximenko and Niiler have used this smooth MDT to parameterize the Ekman dynamics, i.e., the imbalance between the three first terms of their equation, to the local NCEP wind at 10 m level. In addition, they used a new variational technique to downscale the smooth MDT with their estimates of the MDT gradient. Weights of the costfunction are tuned so that their product deviates significantly from the MDT of V. Zlotnicki only at scale less then 1000 km, where drifter data are available. Effective smoothing scale is set at 0.5°, which is also the spatial resolution of the grid. The reference level of the dynamic topography was then changed by subtracting the global mean of the MDT. The MDT and an additional description of its processing are available at http://apdrc.soest.hawaii.edu/projects/DOT/. The data set also provides a mask of drifter data distribution, which is not applied in this study. It should be noted that low-pass filtering of the Maximenko-Niiler MDT will increase the influence of the MDT of V.Zlotnicki and reduce the impact of drifter data.

2.6. Comparison of Observational Mean Dynamic Topographies

[19] The Rio05 estimate is illustrated in Figure 1. This estimate is chosen as a reference, as this MDT includes the most observational information. The fact that Rio05 is displaced to match the *Levitus et al.* [1998] dynamic topography relative to 1500 m, causes an offset in the difference fields of 1.16 m (with respect to Chambers-Zlotnicki and Naeije), 1.62 m (Maximenko-Niiler) and 1.52 m (LeGrand). These biases are completely arbitrary, and they do not affect the determination of geostrophic currents which are computed from MDT gradients. In the comparison that follows, either the offset between the different MDTs has been removed or the MDTs have been considered regionally relative to an area mean.

[20] Although most of the MDTs include observations from the same satellites, it should be noted that differences between MSS can be considerable. An extensive comparison of three MSSs fields illustrates that RMS differences between MSS are in the 2.5–3 cm range for that part of the ocean which is deeper than 500 m [*Hernandez and Schaeffer*, 2001]. Regional differences can reach values up to 8 cm in energetic regions such as the Gulf Stream, the Kuroshio, the Agulhas retroflection and the ACC. The two most widely used MSSs, the CLS01 MSS [*Hernandez et al.*, 2001] and the GSFC 00.1 MSS [*Wang*, 2001], have different periods for reference (CLS01: 1993–1999, GSFC MSS 00.1: 1993–1998). As a consequence, differences are likely to be due to residual interannual variability. The spatial structure of the difference between the two MSSs reveal El Niño/La Niña-like variability in the tropical Pacific and mesoscale variability in the WBC regions. In addition to this, MSS errors are known to be high in coastal regions, where altimeter satellite tracking tends to be worse. Rms differences between MSSs can be as large as 10 cm in regions where the ocean is shallower than 100 m. Finally, considerable differences between MSS fields can occur as a result of differences in altimeter data processing (for example, inverse barometric correction, electromagnetic bias correction). The differences in MSS, but also the differences in the averaging periods of in situ data used for the MDTs should be kept in mind when comparing the different products.

[21] Differences between the two estimates which do not include oceanic in situ observations (Chambers-Zlotnicki and Naeije) are concentrated in coastal regions, where they may exceed the 5 cm level (not shown). Outside of these regions, the correspondence is very good. This is not surprising, as both estimates are based on the same altimeter data and geoid models. The differences in the coastal regions are likely to be related to the strong coastal gradients in the Naeije MDT, which are caused by the transition of the MDT to the EGM96 geoid at land points. These gradients reflect the differences between the EGM96 geoid and the GGM02c geoid, and should not have been

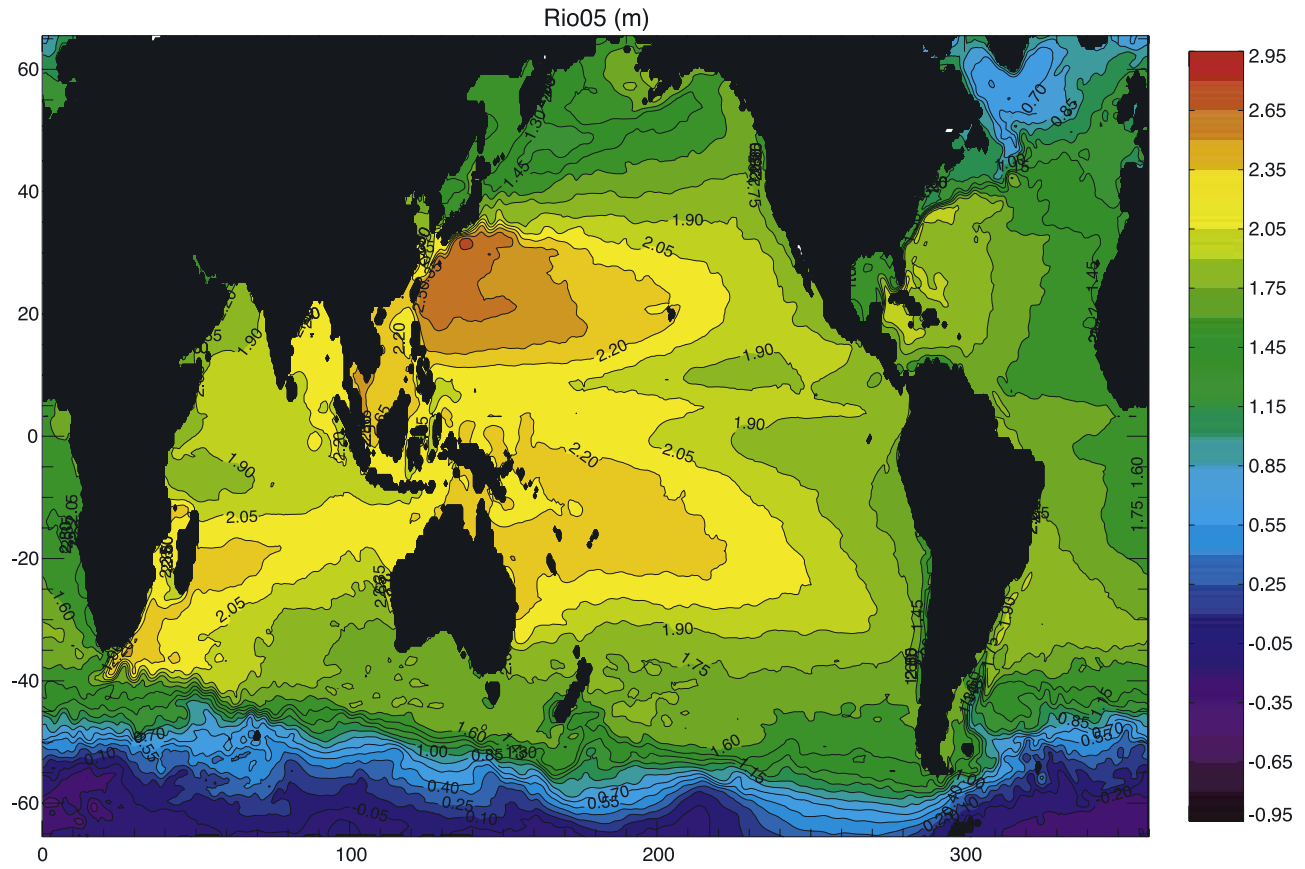

Figure 1. Observational MDT Rio05, contour interval is 15 cm.

present if the grid points at land would have been set to the GGM02c values (M.C. Naeije, personal communication, 2006). The remainder of differences between Chambers-Zlotnicki and Naeije are likely to be due to differences in the MSS and the filtering of the MSS minus geoid difference field.

[22] The difference between LeGrand and the other observational MDTs suggests that the LeGrand MDT is too low in the Indian Ocean and ACC, and too high in the Atlantic and Pacific Oceans (not shown). In addition, this MDT exhibits a meridional bias, where the MDT in the tropical regions is relatively higher than in other solutions. This pattern is also present in the comparison with model-based MDT estimates. Although the bias suggests an overestimation of the subtropical gyre circulation, the transports computed in the inverse model of the LeGrand MDT have realistic values (P. LeGrand, personal communication, 2006). The cause for this bias is unclear.

[23] Small-scale differences between the observational MDTs reflect uncertainties in both MSS and geoid, as well as differences in observational information. This is illustrated in Figure 2, which shows the original MDTs in the Agulhas retroflection area. The LeGrand MDT has the weakest gradients in sea level as a result of its coarse resolution. The Chambers-Zlotnicki and Naeije MDTs are very similar, but processing differences between the two MDTs result in slightly stronger gradients in the Naeije MDT. This is not only the case in places where we expect gradients to be strong (in the Agulhas proper and return current) but also along the African coast, north of 30°S, and the island of Madagascar. As discussed above, these gradients are due to the transition of the MDT to the EGM96 geoid at land.

[24] In the Rio05 and the Maximenko-Niiler MDTs the gradient of the Agulhas current along the African coast is relatively weak, but the gradient of the return flow, and its meandering spatial structure, are more pronounced than in the other MDTs. The comparison suggests that the in situ observations sharpen the fronts in the MDT, not only in the Agulhas, but also in other western boundary currents (WBCs) and the Antarctic Circumpolar Current (ACC, not shown). That this sharpening is not visible in the MDTs based on altimetry only, is probably related to the smoothing applied to reduce geoid errors.

[25] Also in the Gulf Stream region the inclusion of in situ data results in sharper gradients (not shown). Again, the Rio05 and the Maximenko-Niiler MDTs have the strongest sea level gradients. The position of the Gulf Stream is identical in all five observational MDTs. Around 59°W, the Rio05 solution has a meandering structure. This meander is only weakly visible in the Maximenko-Niiler MDT, but is lacking in the other three observational MDTs, similarly to what is observed for the Agulhas return current. This type of Gulf Stream meanders has been observed in the yearly mean positions of the Gulf Stream Landward Surface Edge based on satellite infrared radiometry analysis of *Auer* [1987], but they are not present in his 5-year climatology.

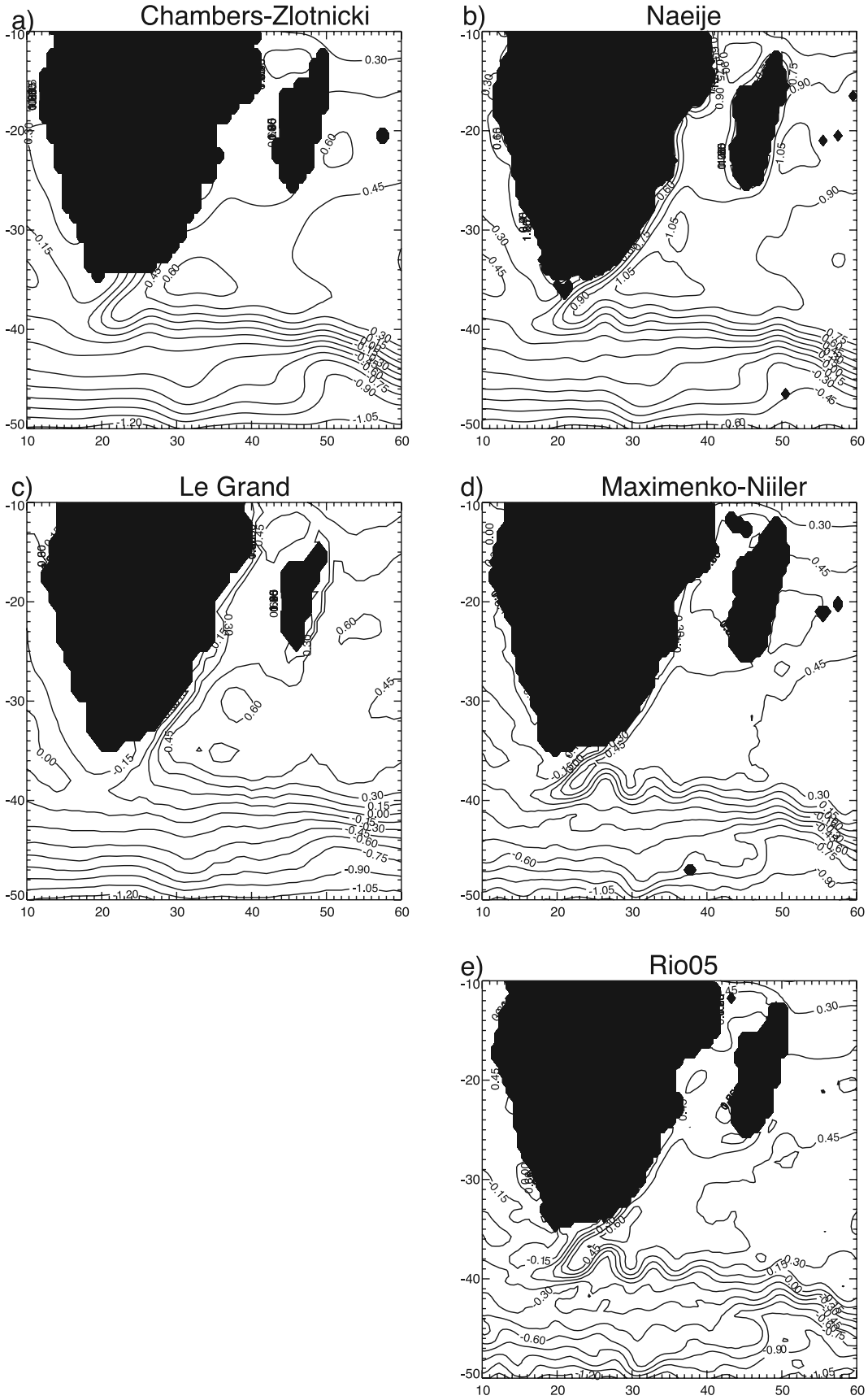

Figure 2. Observational MDTs in the Agulhas region: (a) Chambers-Zlotnicki, (b) Naeije, (c) LeGrand (d) Maximenko-Niiler, and (e) Rio05. Contour interval is 5 cm. Area means are subtracted.

Table 2. Overview of Model-Derived Dynamic Topographies

MDT	Model	Resolution	Period	Forcing
ORCA	Océan Parallelisé	1/3°–2°	1951–1999	NCEP
MPI-OM	Max Planck Institute- Ocean Model	15–184 km	1948–2002	NCAR/NCEP
OCCAM	OCCAM	1/4°	1985–2003	NCEP
POP	Parallel Ocean Program	0.1°	1998–2000	NCEP
HYCOM	Hybrid Coordinate Ocean Model	1/12°	ERA-15 Clim.	ECMWF
ECCO	MITgcm	1°	1992–2004	NCEP
NCOM	Naval Coastal Ocean Model	1/8°	1998–2005	NOGAPS

This suggests that such a meander is a transient feature of the Gulf Stream.

3. Model Estimates of the Mean Dynamic Topography

[26] Seven state-of-the-art OGCMs each with its own discretizations and formulations for oceanic (mixing) processes, provide different global solutions of the mean sea level. Different atmospheric forcing fields have been used for the models, and the averaging period varies. Nevertheless, the time-averaged sea level fields are regarded as "climatological" descriptions of the MDT. An overview of the different models and their resolutions is given in Table 2, and their setup is described in the following subsections.

3.1. ORCA

[27] ORCA2.0 is a global configuration of the Océan Parallelisé (OPA) of the Laboratoire d'Océanographie et de Climatologie (LODYC, now: Laboratoire d'Océanographie et du Climat-Expérimentation et Analyse Numérique LOCEAN) with a resolution of roughly 2, getting smaller to 1/3° near the equator. ORCA is the generic name given to global ocean configurations using OPA model. The model has 31 levels in the vertical, and a free-surface formulation [*Roullet and Madec*, 2000]. Vertical eddy diffusivity and viscosity coefficients are computed from a 1.5 turbulent closure scheme [*Blanke and Delecluse*, 1993]. Enhanced vertical diffusion is applied to remove statically unstable density profiles [*Lazar et al.*, 1999]. Lateral diffusion is modeled along isopycnals, using a horizontal filtering of the isopycnals prior to the computation of the isopycnal diffusion operator. The filtering avoids the need for a minimum background horizontal diffusion for numerical stability. In addition to this, a *Gent and McWilliams* [1990] quasiadiabatic parameterization is used, in which eddy-induced advection is added to the tracer equation to mimic mixing caused by baroclinic instabilities.

[28] Further details of the model are given by *Madec et al.* [1998]. The model has been run for a period of 49 years (1951–1999) (K. Rodgers, personal communication, 2004), forced with NCEP atmospheric fields [*Kalnay et al.*, 1996]. The MDT is computed from this run by time-averaging the sea level over this period.

3.2. OCCAM

[29] The OCCAM (Ocean Circulation and Climate Advanced Modeling) model is based on the Bryan-Cox-Semtner OGCM [*Bryan*, 1969; *Semtner*, 1974; *Cox*, 1984]. Details are described by *Coward and de Cuevas* [2005] and *Webb et al.* [1998]. The model has 66 levels in the vertical. To overcome problems of convergence near the North Pole, the grid is split into two parts. The model uses a K-Profile Parameterization (KPP) mixing scheme [*Large et al.*, 1994], and isoneutral mixing, which does not require a background horizontal diffusivity to remain stable [*Pacanowski and Griffies*, 1998]. An additional *Gent and McWilliams* [1990] mixing scheme is used to account for eddy-induced mixing. The model has been run at a 0.25° resolution for a period of 19 years (1985–2003) using the 6-hourly winds and full surface forcing from NCEP including satellite fields as described by *Coward and de Cuevas* [2005].

3.3. HYCOM

[30] In contrast to OPA and OCCAM, the Hybrid Coordinate Ocean Model (HYCOM) includes isopycnic coordinates over most of the water column in deep water, is terrain following in coastal regions, and z-level in the surface mixed layer and in unstratified seas [*Halliwell*, 1998; *Halliwell et al.*, 1999; *Chassignet et al.*, 2003, 2006]. This model evolved from the Miami Isopycnic-Coordinate Ocean Model [*Bleck*, 1998]. Mixing is parameterized with the mixed-layer model of the NASA Goddard Institute for Space Studies (GISS) [*Canuto et al.*, 2004]. A description of the model formulation is given by *Bleck et al.* [2002].

[31] The HYCOM MDT estimate used in our study is based on a 5-year climatological run with a spatial resolution of 1/12°, and 32 layers in the vertical. It is forced with monthly ERA-15 climatology [*Gibson et al.*, 1997] with 6-hourly wind anomalies added. The bulk formula in the heat flux parameterization implies that these wind anomalies cause an additional 6-hourly variability in the heat flux forcing. Since the forcing is identical in all years, features that are a direct response to atmospheric inter annual variability, such as El Niño/La Niña, are absent from the simulation.

3.4. MPI-OM

[32] The Max Planck Institute Ocean Model (MPI-OM) is a z-coordinate OGCM. The mixing parameterization includes isopycnal tracer diffusion following the implementation of *Griffies* [1998]. Eddy-induced tracer transport uses the scheme of *Gent et al.* [1995]. It also includes a bottom boundary layer slope convection scheme [*Legutke and Maier-Reimer*, 2002]. The model contains a free surface and a state-of-the-art sea ice model with viscous-plastic rheology and snow. The MDT analyzed here was generated from a model simulation over the period 1948–2002, that has been forced with NCAR/NCEP forcing. The model has an irregular grid (approximately 1°) and a vertical resolution

of 23 levels. Further details are given by *Marsland et al.* [2003].

3.5. POP

[33] The Parallel Ocean Program (POP [*Dukowicz and Smith*, 1994]) is based on earlier level models by Bryan, Cox, Semtner and Chervin, which also formed the basis for the OCCAM model. Sub-grid-scale mixing is parameterized using biharmonic momentum and tracer diffusivity. The model has a KPP mixing parameterization [*Large et al.*, 1994]. There is no explicit sea ice model or bottom boundary layer parameterization. The model that was used to generate the present MDT has a spatial resolution of 1/10° horizontally and 40 levels vertically. It is forced by daily averaged NCEP reanalysis winds [*Kalnay et al.*, 1996] with heat and fresh water fluxes derived from a mixture of daily and monthly atmospheric state fields. Wind stress and heat fluxes are calculated using the *Large and Pond* [1981] bulk formulae. The model run describes the 1998–2000 period. More details about the model configuration that is used for this simulation are given by *Maltrud and McClean* [2005].

3.6. ECCO

[34] The project of Estimating the Circulation and Climate of the Ocean (ECCO), [*Stammer et al.*, 2002, 2003], assimilates different types of observations into the MITgcm [*Marshall et al.*, 1997]. The ocean model has a resolution of 1° by 1°, 23 levels in the vertical and a full surface mixed layer based on KPP [*Large et al.*, 1994]. KPP comprises a nonlocal term which mimics convection through enhanced mixing under unstable conditions. The assimilation system is based on the adjoint method that uses Lagrange multipliers. The underlying adjoint code is generated by automatic differentiation using the software tool TAF [*Giering and Kaminski*, 1998]. Control variables are initial temperature and salinity, as well as time-dependent surface buoyancy and momentum fluxes.

[35] The present analysis is based on iteration 199 of the so-called version 2 of the ECCO-GODAE production (ECCO-GODAE-v2.199) [see *Wunsch and Heimbach*, 2006, 2007]. It differs from version 1 (which ended with iteration 69, and is referred to as ECCO-SIO-v1.69), in that most observational data sets and weights previously employed [see *Lu et al.*, 2002] have been revised, updated, and the period extended from 2002 to 2004. Assimilated data now incorporate SLA from TOPEX/Poseidon, Jason-1, ERS-1/2, ENVISAT, and an MDT provided by CLS (M.-H. Rio, personal communication, 2006). This MDT is based on the CLS01 MSS and the EIGEN-GRACE03S geoid, which has also been used for the Rio05 MDT, but in contrast to the Rio05, it does not include any in situ data.

[36] In situ data assimilated in the analysis include the WOCE hydrographic sections, Argo as well as P-ALACE floats, and XBT data. Sea surface temperatures are constrained by monthly mean data from *Reynolds et al.* [2002]. The monthly-mean annual cycle of three-dimensional temperature and salinity is fitted to a merged climatology between WOA01 [*Conkright et al.*, 2002] above 300 m and the WOCE Global Hydrographic Climatology [*Gouretski and Koltermann*, 2004] below 300 m. Improvements in prior uncertainty estimates and weights are documented in the papers by *Forget and Wunsch* [2007] and *Ponte et al.* [2007]. The model is forced by 6-hourly NCEP/NCAR air-sea fluxes that have been adjusted by the assimilation. More details are given by *Wunsch and Heimbach* [2006, 2007] as well as the ECCO website (http://www.ecco-group.org).

3.7. NCOM

[37] The Navy Coastal Ocean Model (NCOM) is a free-surface, primitive-equation model based primarily on two other models, the Princeton Ocean Model [*Blumberg and Mellor*, 1987] and the Sigma/Z-level Model [*Martin*, 2002]. The model is run in a resolution of approximately 1/8° [*Barron et al.*, 2006]. Its 40 sigma-z levels are concentrated toward the surface to maintain a minimum rest thickness of 1 m in the uppermost layer.

[38] The atmospheric forcing is obtained from the Navy Operational Global Atmospheric Prediction System (NOGAPS) and the model assimilates temperature and salinity fields with the Modular Ocean Data Assimilation System (MODAS) [*Fox et al.*, 2002]. The assimilation system [*Kara et al.*, 2006] uses sea surface height fields from the high-resolution Navy Layered Ocean Model (NLOM) [*Wallcraft et al.*, 2003], which assimilates observations from the GEOSAT Follow-On (GFO), JASON-1 and ENVISAT satellites. The model does not assimilate an MDT based on altimetry and a geoid model (as is the case in ECCO), but instead, uses a mean sea level based on a high-resolution model run that has been adapted to match the position of the fronts with infrared radiometry [*Smedstad et al.*, 2003]. This has been done by applying several methods including data merging, adapting the extreme values and rubber sheeting [*Carnes et al.*, 1996]. In addition, sea surface temperature observations from multichannel AVHRR are being assimilated. NCOM sea surface height agrees well with tide gauge observations, both in a free running and in an assimilative case [*Barron et al.*, 2006]. The MDT used in this study has been computed from a simulation over the period 1998–2005. A validation of the assimilation and further details are given by *Kara et al.* [2006].

3.8. Comparison of Modeled Mean Dynamic Topographies

[39] Each modeled MDT was delivered at its own model resolution. To obtain comparable fields, the model grids have been converted to a regular 1° grid by spatial smoothing using a Hamming window with a cutoff wavenumber $N = 120$, which corresponds to an effective resolution of 167 km. For a description of this filter, see section 4. Two types of ocean models can be distinguished: those that assimilate observations (ECCO, NCOM), and those that do not (ORCA, MPI-OM, OCCAM, HYCOM, POP). The spread in the nonassimilative models at the given spatial resolution, as presented in Figure 3, gives an impression of the variations in the sea level representation of present-day numerical ocean models. These differences have two main sources: model error (including errors in atmospheric forcing) and differences in averaging period. Largest differences are found in the ACC and the WBC regions. These regions are known to have sharp frontal features. On one hand, the variability associated with these fronts will cause considerable differences in MDT related to differences in averaging period. On the other hand, such

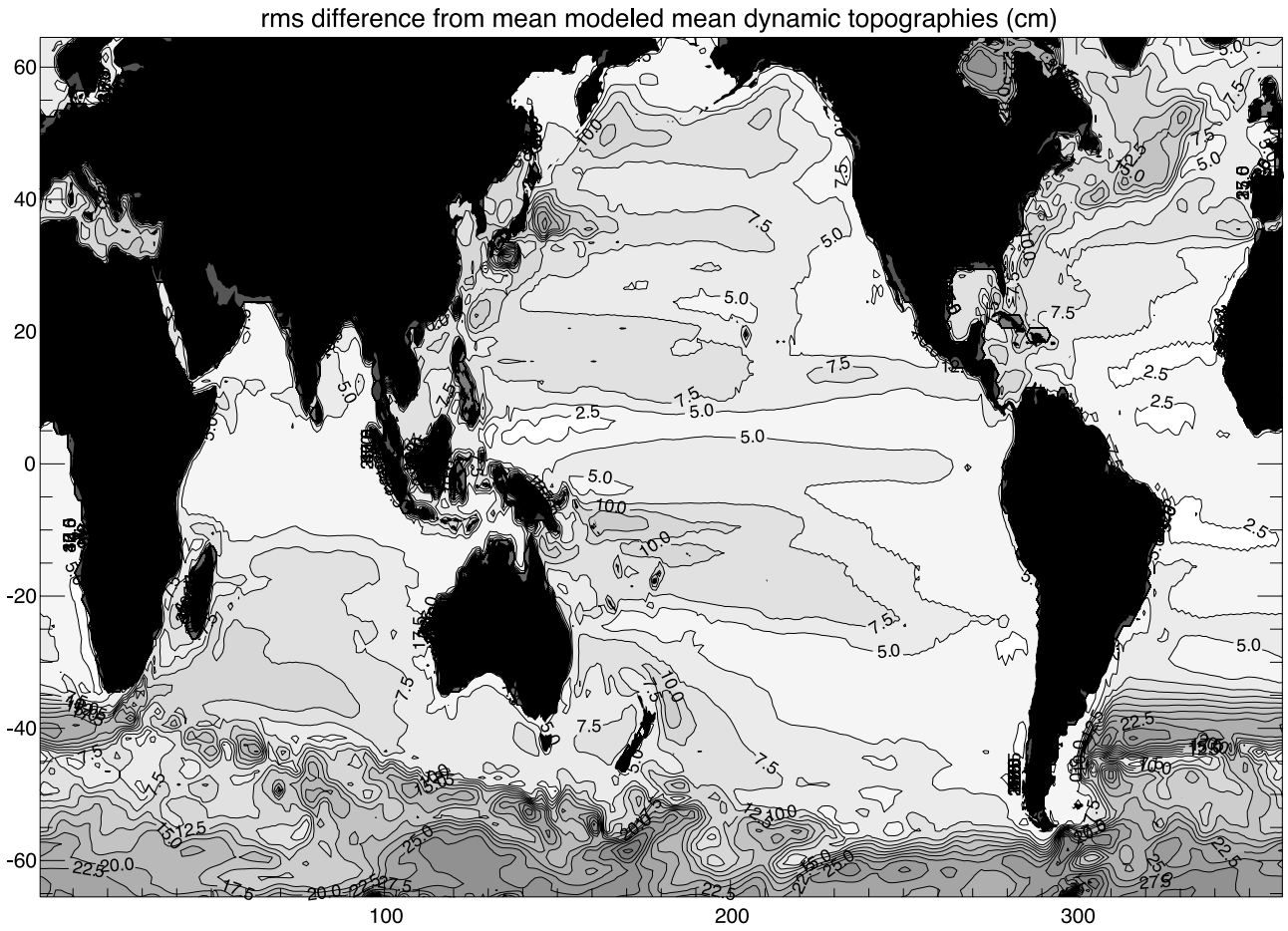

Figure 3. RMS differences from mean as a function of longitude and latitude for the mean dynamic topographies from ORCA, MPI-OM, OCCAM, POP and HYCOM. Contour interval is 2.5 cm, and values larger than 2.5 cm are shaded.

fronts are not always well represented by numerical models owing to limited resolution or other model limitations such as parameterization of mixing, representation of bottom topography and limited vertical resolution. For example, the front associated with the ACC may be overestimated in numerical models by a factor of 2 [*Stammer et al.*, 1996; *Thorpe et al.*, 2005].

[40] MDT differences caused by differences in averaging period are investigated with the time series of the both ECCO and ORCA. The ORCA time series has been divided into four 10-year periods and one 9-year period. RMS differences between the mean sea level fields of these periods are in the 2.5–3 cm range. The time series for ECCO has been split in two periods: 1992–1998 and 1999–2004. The RMS difference of the mean sea level for these periods is 3.6 cm. These results indicate that differences in averaging periods cause nonnegligible differences in MDT.

4. Comparison of the Modeled Mean Dynamic Topographies With the Observational Mean Dynamic Topographies

[41] To investigate the differences between MDT estimates from observations and models at different spatial scales, the small-scale features have been filtered out with a low-pass filter. The choice for a filter requires care. While the geoid is defined over land, the MSS is not, and consequently the MDT is undefined over land. Applying a spectral filter requires the values over land to be filled in (for example, with geoid undulations, zeros, or by zonal interpolation), and this may introduce additional errors in the filtered field. Therefore a spatial filter has been chosen to smooth the MDTs considered in this study.

[42] Many spatial smoothers, or low-pass filters, are based on the Gaussian function. This function has the advantage that the frequency response function is well known, but the disadvantage that it tends to attenuate the low-frequency signals while suppressing the high-frequency ones (results not shown). Following the approach of *Jayne* [2006], a Hamming window smoother has been applied, which is given by the equation

$$F(\gamma) = \begin{cases} 0.54 + 0.46\cos(N\gamma) & \gamma \le \pi/N \\ 0 & \gamma > \pi/N, \end{cases} \quad (1)$$

where γ is the angle between two points (θ_1, ϕ_1) and (θ_2, ϕ_2) on the surface of the Earth, given by $\cos\gamma = \sin\theta_1 \sin\theta_2 + \cos\theta_1 \cos\theta_2 cos\,(\phi_1 - \phi_2)$ and N is a wavenumber. The reasons for using this smoother are clearly described by

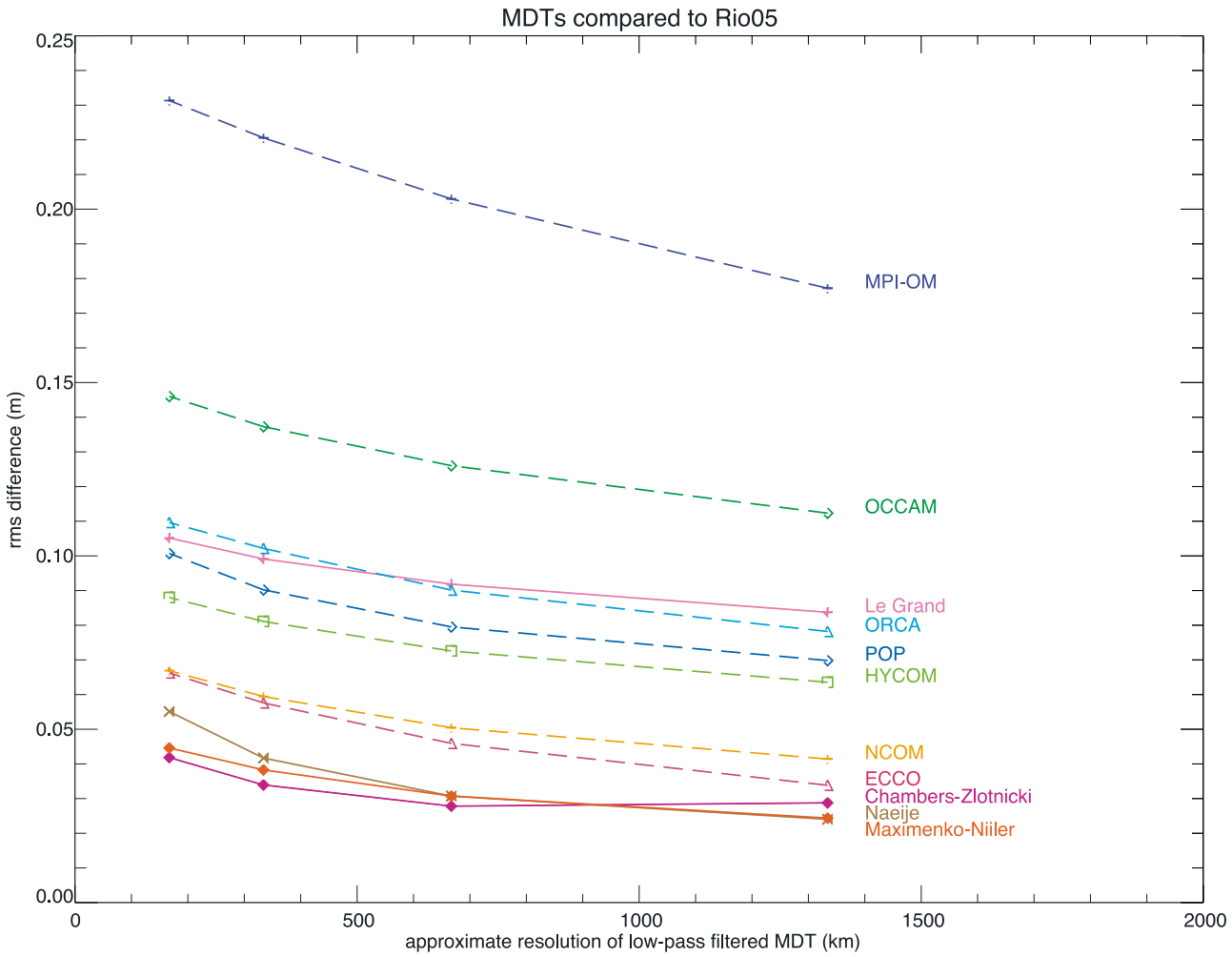

Figure 4. RMS differences between the different MDTs and the reference MDT Rio05 as a function of the cutoff wavelength of the low-pass filter. Model MDTs are indicated with dashed lines.

Jayne [2006] and are repeated here. The main advantage of using this filter to using a Gaussian is that it has a well-defined cutoff wave number in the spectral domain, while the Gaussian function has nonzero values over all frequencies. In addition, it minimizes the sidelobes in the wave-number domain. A practical advantage is that the Hamming window has a finite domain, while the Gaussian function includes all points on the sphere.

[43] The cutoff wave number is given by the value of N. At a wavenumber of $2N$, the power spectrum of the filter trails off to zero. The approximate resolution (Δ) of the low-pass filtered field is given by:

$$\Delta = \frac{2\pi \cdot R_{Earth}}{2N}, \qquad (2)$$

where R_{Earth}, the radius of the Earth, is set to 6371 km. Points over land have been disregarded from the smoothing. This may cause errors near the coast, but this approach is preferred to filling in land points with zeros or some other value such as those derived from a geoid model. The MDTs have been filtered at four different wave numbers, corresponding to four different spatial resolutions: N = 15 (Δ = 1334 km), N = 30 (Δ = 667 km), N = 60 (Δ = 334 km), and N = 120 (Δ = 167 km). In this comparison, only the MDT equatorward of 65.5°N and 65.5°S has been considered.

[44] As a reference for further comparisons, the Rio05 MDT has been chosen, as it includes most in situ observations. An overview of the RMS differences as a function of the approximate spatial resolution of the Hamming window smoothed field is presented in Figure 4. The low RMS differences for the Chambers-Zlotnicki and Maximenko-Niiler MDTs (ranging from 4.2 cm and 4.5 cm at N = 120 to 2.9 cm and 2.4 cm at N = 15) indicate a strong resemblance to Rio05. Differences with Naeije MDT are slightly larger, mostly owing to its gradients in coastal regions. The LeGrand MDT differs from Rio05 by 11 cm (at N = 120) to 8.3 cm (N = 15) RMS, as a result of the large-scale differences and the weaker gradients as discussed in section 2.6.

[45] It should be noted that RMS differences when choosing the Chambers-Zlotnicki or Maximenko-Niiler as a reference MDT were not substantially different from those presented in Figure 4. This confirms the observed similarity between the Rio05, Maximenko-Niiler and Chambers-Zlotnicki topographies. It also implies that differences in number and type of in situ observations that

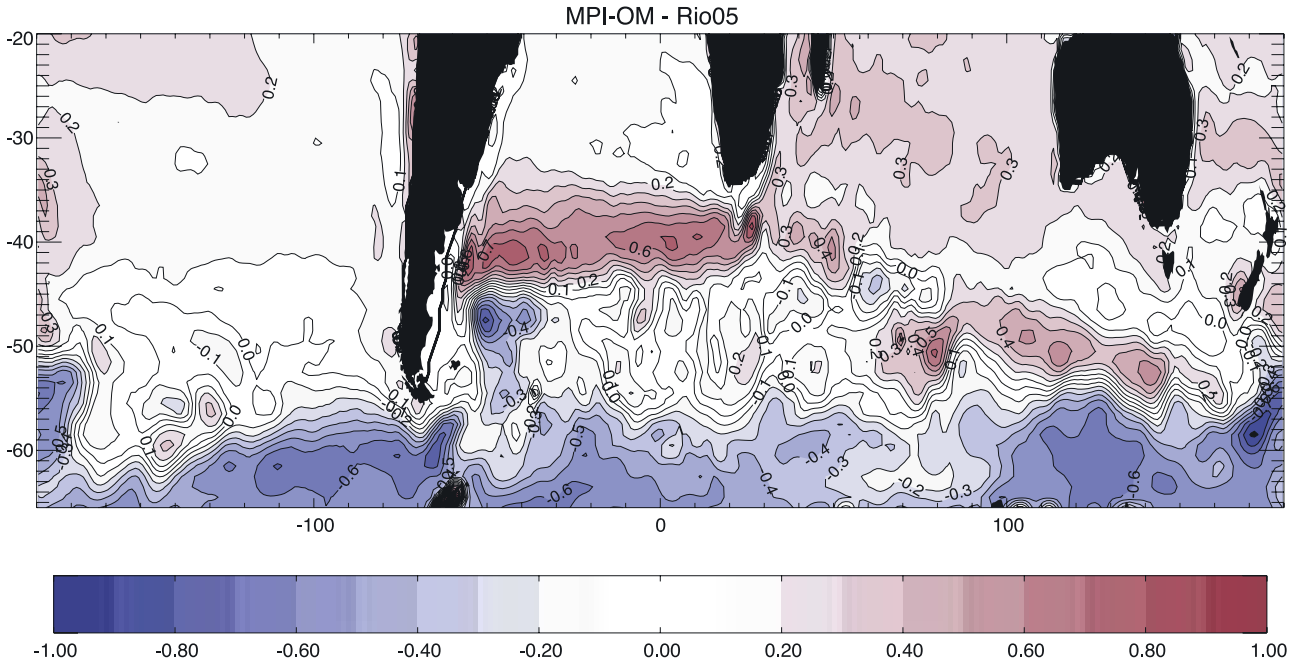

Figure 5. Difference between MPI-OM and Rio05 MDTs after low-pass filtering with a Hamming window using $N = 120$. Contour interval is 10 cm, and differences larger than 10 cm are shaded. The area mean difference has been removed.

mostly affect the small scales, as well as the differences in averaging period of the MSS, have an impact on the dynamic topography that remains below the 5-cm RMS level.

[46] Low-pass filtering with the Hamming-window smoother reduces differences between the MDTs, but does not lead to qualitatively different results. Generally speaking, the largest differences between the MDTs are found in the WBC regions and in the ACC. While differences in the representation of the strong gradients associated with WBCs and the ACC are reduced with increasing filtering scales, the differences in gyre strength remain visible (not shown). In particular the subtropical gyre in the North Atlantic is weaker in the modeled MDTs than in Rio05. In addition, the models have a Gulf Stream whose path is more zonal and a Kuroshio position further North than observed. In all models without data assimilation, the ACC is stronger than in the Rio05 MDT.

[47] The reduction in RMS differences with increasing spatial filtering scale, as illustrated in Figure 4 is only a few centimeter for OCCAM, ORCA, POP and HYCOM. Contrary to the common perception that large-scale ocean circulation is reasonably well known, this result suggests that uncertainties at the larger spatial scales are not much smaller than uncertainties at the smaller scales. Consequently, a further reduction of uncertainties in the mean dynamic topography through reduced MSS errors, improved geoid accuracy and/or numerical model refinement can be expected over the entire $N = 15-120$ wavenumber range.

[48] The results for the observational MDTs are all similar, with the exception of the LeGrand MDT. The major difference between this MDT and the other observational MDTs is the choice of the EGM96 geoid, instead of some GRACE-derived geoid. This is a plausible cause for the exceptionally large differences between the LeGrand MDT and the Rio05 MDT.

[49] Not surprisingly, largest differences have been found between the reference MDT and the ocean models that do not assimilate observations. In particular, the MPI-OM MDT deviates strongly from the Rio05 MDT, ranging from 23.1 cm RMS at $N = 120$ to 17.7 cm at $N = 15$. Differences are concentrated in two regions, where they reach values around 50 cm: the Southern Atlantic Ocean (ACC and Brazil-Malvinas confluence) and the Gulf Stream. The differences in the Southern Ocean are illustrated in Figure 5, indicating that the Agulhas leakage in the MPI-OM MDT is represented as a continuation of the subtropical gyre in the Indian Ocean that traverses the South Atlantic. This points to a circulation that is more viscous than the observed circulation (see also the discussion by *Dijkstra and de Ruijter* [2001]). The low resolution of MPI-OM and the choice of mixing coefficients may be held responsible for this. The differences between MPI-OM and Rio05 in the Gulf Stream region are related to the Gulf Stream separation point, as will be discussed later.

[50] The ORCA MDT, in spite of its low horizontal resolution, agrees reasonably well with the Rio05 MDT. Largest differences are found in the ACC region, as well as the Gulf Stream and Kuroshio regions (not shown). In contrast to the MPI-OM MDT, the ORCA MDT has an Agulhas leakage which is smaller than in Rio05. Likely candidates for this difference are a strong effect of bottom topography, which causes an early retroflection of the Agulhas current and the coarse resolution which inhibits the simulation of eddies. Differences of the ORCA MDT with respect to the Rio05 MDT range from 10.5 cm RMS at $N = 120$ to 7.8 cm RMS at $N = 15$. ORCA has a remarkably

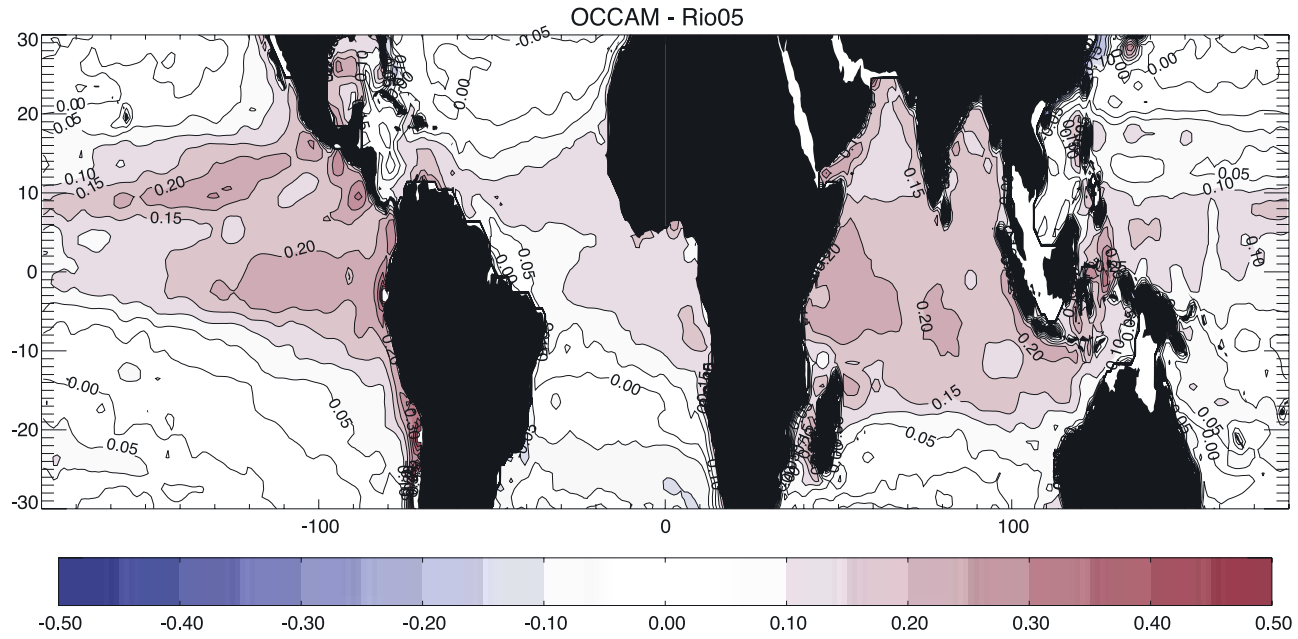

Figure 6. Difference between OCCAM and Rio05 MDTs after low-pass filtering with a Hamming window using $N = 120$. Contour interval is 5 cm, and differences larger than 5 cm are shaded. The global mean difference has been removed.

good correspondence with Rio05 in the tropical band, where spatial resolution of the model is increased.

[51] Differences between the POP MDT, which has a resolution of 0.1°, and Rio05 MDT are only slightly smaller than the differences between the ORCA and Rio05 MDTs and have a more noisy spatial character. Largest differences between POP and Rio05 occur at the North Atlantic Current, near the Kuroshio and in the ACC region.

[52] In addition to differences in the WBC and ACC regions, the OCCAM MDT exhibits relatively large differences with respect to the Rio05 MDT in the tropical band. This is illustrated in Figure 6, which shows the difference between the OCCAM and Rio05 MDTs. Both the Atlantic and the Pacific Ocean have positive sea level anomalies up to 20 cm in the eastern side of the ocean basin, centered around 5°S and 10°N. A similar positive anomaly is visible in the Indian Ocean around 10°S. These features, reminiscent of Rossby waves, may be related to the choice of the wind-stress fields (B. de Cuevas, personal communication, 2006). Together with differences at higher latitudes, they cause the RMS difference with respect to Rio05 to lie in the 10–15 cm range.

[53] Of all the nonassimilative ocean models, only the HYCOM model, which has the highest spatial resolution, has RMS differences from Rio05 that remain below the 10-cm level (8.8 cm at $N = 120$ to 6.4 cm at $N = 15$). This is mostly due to the close agreement between HYCOM and Rio05 in the WBC regions. In the ACC region, however, there are still considerable differences between HYCOM and Rio05, as will be discussed later in this section. In the western and central tropical Pacific, specifically around 10°S, small differences occur that may be a result of missing interannual variability in the HYCOM simulation. HYCOM is forced with climatological winds for the ERA-15 period (1978–1994), while the Rio05 has 1993–1999 as a reference period.

[54] The two models that assimilate observations, NCOM and ECCO, have MDTs that closely resemble the Rio05 MDT (results not shown). At $N = 120$, the RMS differences with Rio05 are 6.6 cm, while at $N = 15$, this is reduced to 4.1 cm. The agreement of these model solutions with Rio05 is good, as they are partly based on the same observations. The ECCO representation of the Kuroshio agrees better with Rio05 than the NCOM MDT. In the ACC region, ECCO has some considerable differences with Rio05 around Drake Passage and the Brazil-Malvinas confluence, while NCOM has larger differences in the Agulhas return current. The difference of ECCO with respect to Rio05 are largest in the ACC region, where the assimilation system assumes the largest uncertainties of the assimilated dynamic topography. This estimate of uncertainties is based on sampling variance of the altimeter, the inverse barometric corrections, and the electromagnetic bias, which is related to significant wave height (P. Heimbach, personal communication, 2006). As a consequence of the increased altimetric uncertainties in this region, the in situ observations will obtain relatively higher weight in the assimilation. Note that, in contrast to Rio05 and Maximenko-Niiler, no drifter observations have been included in the present ECCO estimate. The effect of the higher resolution in NCOM on the differences with Rio05 is not noticeable in this comparison. As the estimates are not independent, interpretation of these differences remains limited.

4.1. Gulf Stream

[55] The separation of the Gulf Stream is more northerly in most model estimates than it is in the observational MDTs. As an independent reference, the estimates of the models without data assimilation have been compared to the

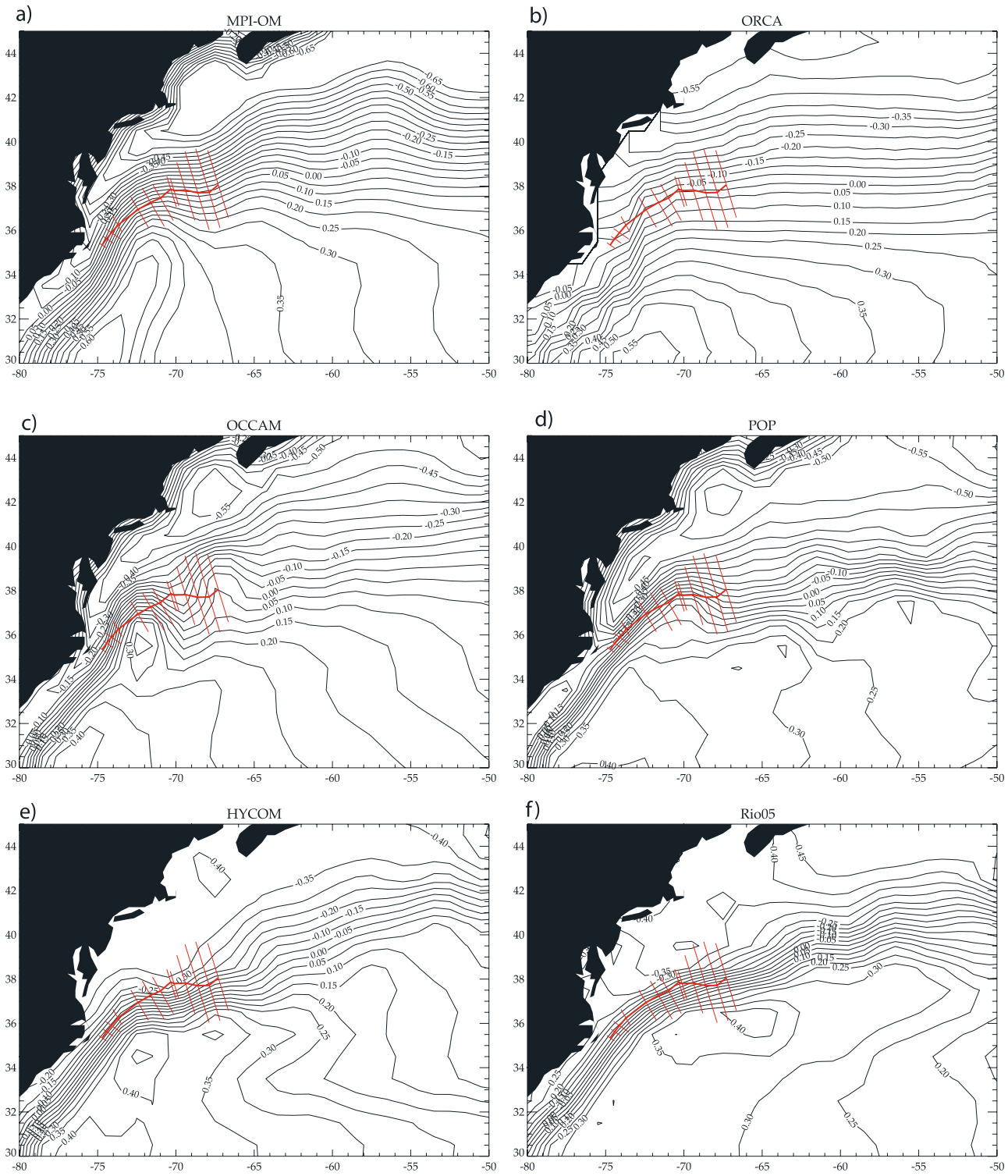

Figure 7. Modeled MDTs: (a) MPI-OM, (b) ORCA, (c) OCCAM, (d) POP, and (e) HYCOM after low-pass filtering with a Hamming window using $N = 120$. The Rio05 MDT is given for reference (bottom right). Contour interval is 5 cm. The mean position (thick line) and standard deviation (thin lines) of *Watts et al.* [1995] are indicated in red. Area means have been removed.

mean path of the Gulf Stream from the analysis of *Watts et al.* [1995], which is illustrated in Figure 7. The overshoot of the Gulf Stream near the separation point is most clear for MPI-OM and OCCAM. Both models have a Gulf Stream that is more northerly compared to the observed mean path. The Gulf Stream in ORCA is more diffuse owing to its low resolution.

[56] *Smith et al.* [2000] illustrated that the simulation of the separation of the Gulf Stream is resolution-dependent and demonstrated a transition of regimes between 0.1°

Table 3. RMS Differences Between the Modeled MDTs and the Rio05 MDT in the Southern Ocean[a]

MDT	RMS Difference
MPI-OM	30.7
ORCA	15.0
OCCAM	15.5
POP	10.5
HYCOM	8.4
ECCO	7.7
NCOM	6.7

[a]Southern Ocean is 65°S to 20°S; values are given in centimeters.

and 0.2° resolution. The Gulf Stream in the POP MDT, which is generated with a resolution of 0.1°, agrees relatively well with the observed mean path. Also its tightness near the coast and the weakening of the gradient off-stream is consistent with the observed standard deviation in the Gulf Stream mean path. HYCOM is the only model whose path is more southerly between 75°W and 70°W than the observed mean path. Its continuation east of 70°W is more northerly than other models and closer to the Rio05 MDT.

[57] In all model estimates, the Gulf Stream path is more zonal than in the observational MDTs. This effect is strongest in MPI-OM (up to 55 cm sea level difference with Rio05 MDT) and weakest in HYCOM MDT (20 cm difference with Rio05 MDT). This result suggests that also the representation of the Gulf Stream path improves with increasing resolution.

4.2. Antarctic Circumpolar Current

[58] Largest differences between modeled MDTs are found in the Antarctic Circumpolar Current. This highly energetic current is associated with sharp sea level gradients [*Gille*, 2003] whose simulation requires a high model resolution. As mentioned before, numerical models have shown to overestimate the transport and related sea surface

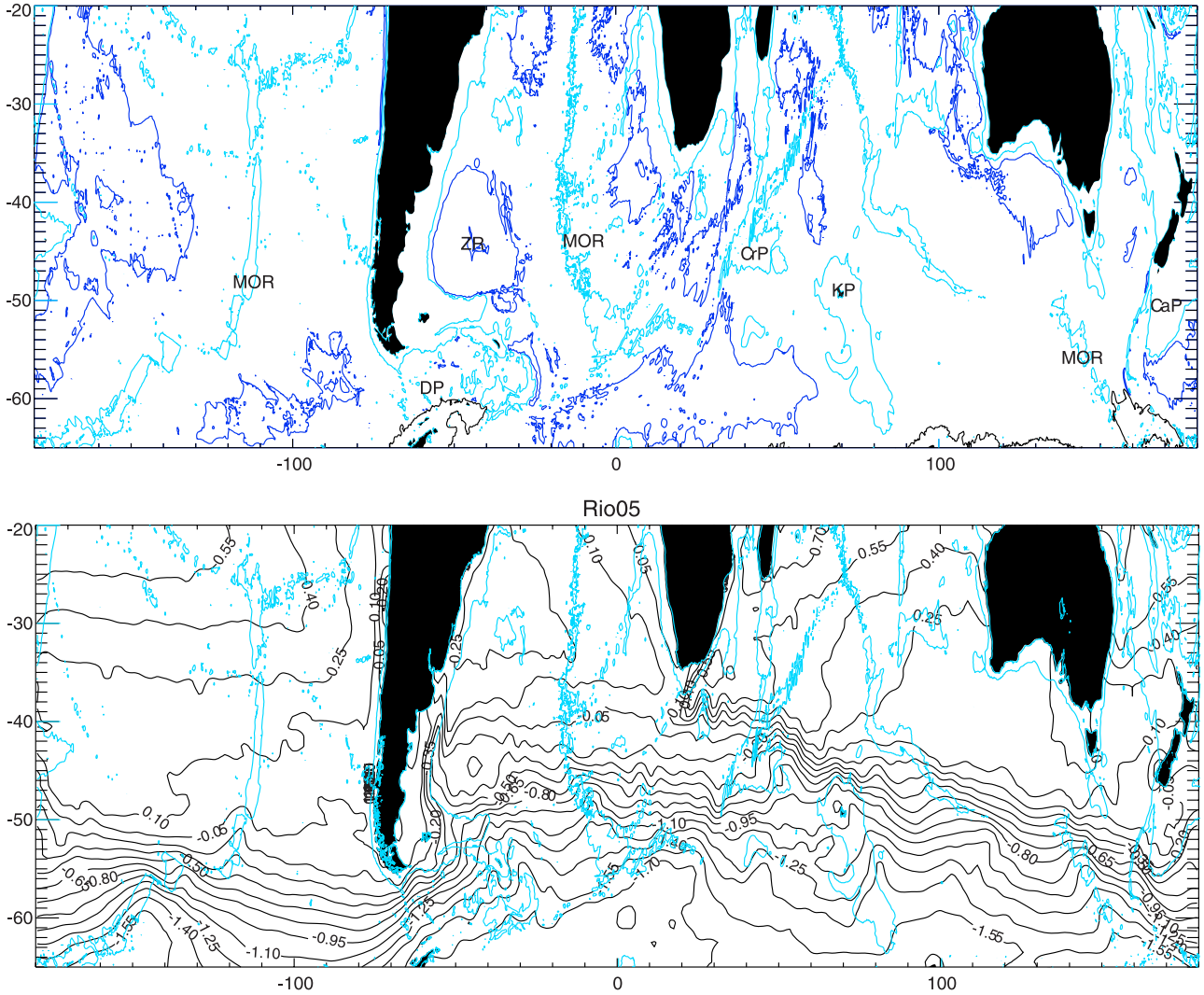

Figure 8. (top) Bathymetry in the Southern Ocean. Bathymetric contours at 5000 m depth are indicated in purple, and at 3000 m are indicated in cyan. (bottom) Rio05 mean dynamic topography (black) and bathymetric contours at 3000 m (cyan). Topographic features indicated are the Mid-Ocean Ridge (MOR), Drake Passage (DP), Zapiola Rise (ZR), Campbell Plateau (CaP), Crozet Plateau (CrP), and Kerguelen Plateau (KP).

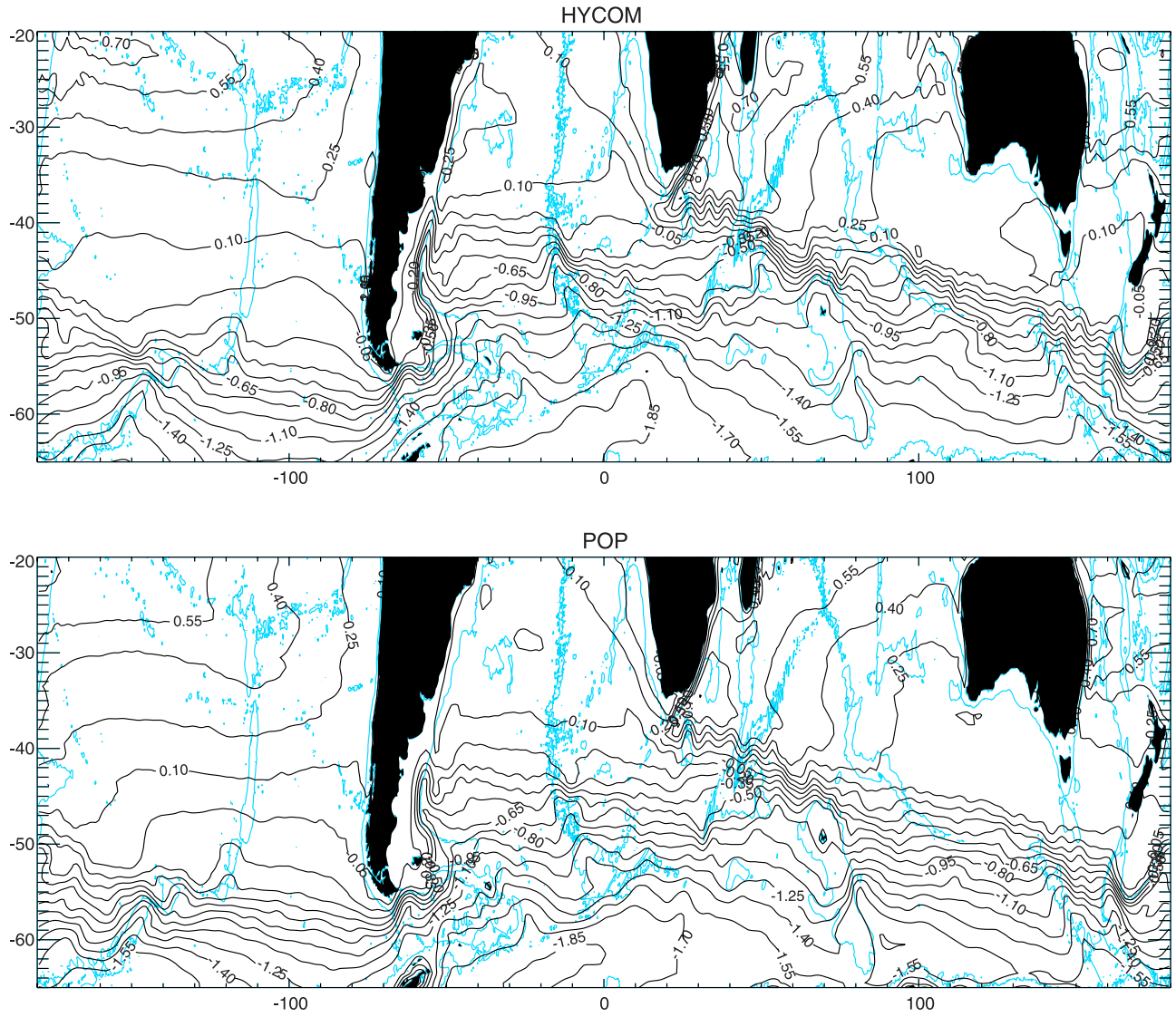

Figure 9. MDTs in the Southern Ocean: (top) HYCOM and (bottom) POP. Bathymetric contours at 3000 m depth are indicated in cyan.

slope up to a factor of 2 [*Stammer et al.*, 1996; *Thorpe et al.*, 2005]. The ACC region, with its sharp fronts, is quite sensitive to differences in averaging period. Although the geoid in this region is relatively accurate at the large scales as a result of the denser ground track coverage of the GRACE satellite, observational MDT errors may be relatively large. This is because the high levels of significant wave height in this region imply larger errors in the electromagnetic bias correction of the altimeter data. By contrast, the topographic features derived from drifter data may be relatively accurate. For example, *Hughes* [2005], who used the Maximenko-Niiler topography to compute the surface vorticity balance of the ACC, demonstrated the high quality of this drifter-based MDT in the ACC region.

[59] An overview of the RMS differences with respect to the Rio05 MDT for the Southern Ocean (20°S to 65°S) is given in Table 3. The large difference between Rio05 and MPI-OM is related to the overestimated Agulhas leakage that has been discussed above. The ORCA ACC has a mean path which corresponds to the observations, but is much smoother owing to its limited resolution. The OCCAM MDT has an MDT slope associated with the ACC which is in places much steeper than the corresponding slope in the Rio05 ACC. In particular the gradient at Drake Passage is relatively strong and exhibits a meandering feature around the Falkland Plateau. This model artifact has also been observed by *Thorpe et al.* [2005].

[60] The high-resolution models POP and HYCOM show a good general agreement with the Rio05 MDT and also correspond with *Gordon et al.* [1978]; *Gordon and Molinelli* [1986]; *Olbers et al.* [1992], but noticeable differences occur in the details. Because of its strong gradient, a relatively small difference in position of the ACC can cause considerable errors between two MDTs. To illustrate the representation of the ACC in the MDTs, the Rio05, HYCOM and POP MDTs are illustrated in Figures 8 and 9. The high-resolution models HYCOM and POP have sea level fields in the Southern Ocean that are relatively close to the Rio05 topography (HYCOM: 8.4 cm RMS, POP: 10.5 cm RMS). As the ACC is

topographically steered [e.g., *Gille*, 2003], it is interesting to see the differences between the z-level POP model and the HYCOM model with isopycnal coordinates. While topographic ridges cause vigorous mixing in z-level models [*Lee et al.*, 2002], this is not the case in isopycnal models, where the transport occurs along isopycnic coordinates by construction.

[61] A number of topographic features (indicated in Figure 8) can be recognized in the sea level fields of both models. The contraction of the dynamic topography contours at the Mid-Ocean Ridges in the Pacific and the Atlantic basins in the Rio05 MDT is weaker than in both model MDTs. South of Australia, the HYCOM MDT has a frontal structure following the course of the Mid-Ocean Ridge in accordance with the Rio05 topography. This gradient is less visible in the POP MDT.

[62] The tight focus of height contours and the meandering structure around the tip of South America is present in both models. Farther north, the anticyclonic circulation at the Zapiola rise [e.g., *Fu*, 2006] is clearly reflected in the Rio05 MDT. Although observable in all MDT estimates which include altimetry, this circulation is missing in all model MDTs without data assimilation. The rise in sea level associated with the Crozet Plateau is weaker in HYCOM than in POP. Both models have a positive height anomaly on the Kerguelen Plateau which is stronger than in Rio05. The ACC in both models deflects southward when it meets the Campbell Plateau south of New Zealand. This causes a tightening of the height contours which is only weakly visible in the Rio05 MDT.

[63] Largest differences between the two models are observed along the Mid-Ocean Ridges near 5°W and southwest of Australia (not shown). In these regions, the HYCOM MDT is generally closer to the Rio05 MDT than the POP MDT. The reasons for this difference is not easily identified, as it may be related to the vertical discretization, but could also be caused by differences in averaging period and the fact that HYCOM is forced by climatology, while POP is not. It should be noted that atmospheric forcing in this region is relatively unconstraint by observations, which may cause considerable errors in the modeled MDTs. The interpretation of the differences is further complicated by the relative large errors in observational MDTs. From the above analysis it is concluded that, with the exception of the Zapiola Rise, the modeled MDTs exhibit a stronger response to topographic features in the ACC than expected from observations.

5. Summary and Discussion

5.1. Summary

[64] Five observational and seven model estimates of mean dynamic topography (MDT) have been compared. Agreement between the observational MDTs is relatively good. The MDT of *Rio and Hernandez* [2004] and *Maximenko and Niiler* [2004] have finer spatial structures as a result of the inclusion of in situ observations. The MDT of *LeGrand et al.* [2003] exhibits large-scale discrepancies and has weaker gradients than the two other MDTs that include in situ observations. The two altimeter-based MDTs, by Naeije and Chambers-Zlotnicki, are based on the same geoid model (GGM02c), but differ in the mean sea surface used, and the processing methodology. While processing differences are most clearly observed in the coastal regions, MSS differences occur over the entire ocean at different spatial scales. Averaging periods of both the altimeter data in the MSS and the additional in situ observations substantially influence the differences between the observational MDTs.

[65] Model estimates can be as close as 8.8 cm RMS to the observational estimates at spatial scales of 1°. This is the case for the high-resolution HYCOM model [*Chassignet et al.*, 2006], which has a relatively close agreement with the Rio05 estimates, particularly in the western boundary current (WBC) regions, where most other models have difficulties representing the sea-level gradients partly because of a limited resolution. In all models investigated here, the representation of the Antarctic Circumpolar Current (ACC) shows largest differences with respect to the observations. The ocean model of MPI-OM [*Marsland et al.*, 2003] differs strongly from the observational estimates, particularly in the South Atlantic. This is probably due to a lack of resolution and high viscosity. In spite of its low resolution, the ORCA model [*Madec et al.*, 1998] agrees reasonably well with the Rio05 MDT. The OCCAM model [*Coward and de Cuevas*, 2005] MDT exhibits remarkable differences with respect to Rio05 in the tropical band. The POP model [*Maltrud and McClean*, 2005] has a Gulf Stream separation which matches the observations. In spite of its high resolution, the POP model has a Gulf Stream which is too zonal, and an overestimated ACC strength. In the ACC region, the HYCOM and POP models have an MDT which is closest to the Rio05 MDT. The MDTs of these two models exhibit a stronger response to topographic features in the ACC than expected from observations. The Zapiola Rise, which is clearly visible in all altimetric MDTs is missing in the MDTs of MPI-OM, ORCA, OCCAM, POP and HYCOM. Two models that assimilate observations, NCOM [*Barron et al.*, 2006] and ECCO [*Wunsch and Heimbach*, 2006, 2007], have MDTs that agree well with the observational estimates, but are not independent.

[66] To investigate the differences at different spatial scales, the MDTs have been low-pass filtered with a Hamming window smoother. Spatial filtering of the MDTs does not affect the results in a qualitative sense. The larger the spatial structures, the smaller the differences between the MDTs. The reduction of differences between MDTs with increasing filtering scales is smaller than expected. While the future gravity mission Gravity Field and Steady-State Ocean Circulation Explorer (GOCE) promises to improve MDT estimates at small spatial scales, a further reduction of errors in the mean sea surface estimates through refined processing of satellite altimetry may be needed to improve MDT estimates at larger scales.

5.2. Discussion

[67] In the present study recent estimates of MDT have been evaluated. Their mutual differences have been quantified, and the regions of largest uncertainties have been identified. Still, this study is not conclusive about the exact errors of the different MDT estimates.

[68] When combining observations from different sources, as is generally the case when estimating an observational mean dynamic topography, the exact error can only

be estimated when all sources of observational errors are taken into account properly. This does not only mean taking into account the instrumental errors, the density of observations, and the covariances between them, but also the difference in spatial scales of the observational information should be considered. In geodesy, the errors resulting from a truncation of spherical harmonics at a certain wavelength, or from low-pass filtering a (geoid) field, are called ''omission errors,'' as opposed to ''commission errors'' that describe the actual errors in the (geoid) field. The omission error is of particular relevance when combining altimetric observations with geoid estimates [*Losch et al.*, 2002]. As a matter of fact, the omission error will also play a role when comparing MDTs of different spatial resolutions as is done in the present study. By low-pass filtering all MDTs to a common resolution, only the commission errors have been considered here.

[69] The reduction of MDT differences with increasing spatial scales is smaller than expected. This implies that the models are relatively far removed from observations at the large scales, where the dynamic topography is assumed to be reasonably well known. This may also imply that the models are already relatively close to the observations at the small scales. It should be realized, however, that given the inhomogeneities in the in situ data applied in the Rio05, LeGrand and Maximenko-Niiler MDTs, and the smoothing applied to the altimeter data, the effective resolution of the observational MDTs may be lower than assumed. Choosing Rio05 as a reference means that we can only judge the model MDT estimates relative to an imperfect ''truth,'' of which the exact error is not known.

[70] In this study, the Rio05 MDT has been chosen as a reference, as it contains the most in situ data. This MDT has more small-scale features than the other observational MDTs. These may be semipermanent ocean features, but may also be caused by aliasing signals with a temporal resolution which is not resolved. The choice for this reference MDT may be somewhat arbitrary, but results obtained with the Chambers-Zlotnicki and Maximenko-Niiler MDTs were qualitatively similar, suggesting that the present findings are robust.

[71] The interpretation of the observational MDT differences is for a large part obscured by the differences in MSS estimates. In part, these can be explained from differences in averaging period, but much of the differences will also be due to errors in altimetric corrections such as the electromagnetic bias correction, the inverse barometric correction and the wet-tropospheric correction. These, together with geographically correlated orbit error, will need to be reduced in order to obtain a more accurate observational MDT. As geoid errors are being reduced by the advances in gravimetry, the processing of altimeter data deserves renewed attention.

[72] At present, observations can only provide a global MDT with reasonable accuracy for scales of 100 km and above. Much of the ocean circulation, specifically mixing processes and vertical circulation, take place on much smaller scales. These processes, which may have a substantial impact on larger-scale circulation cannot be observed with the current satellite techniques. Direct measurements remain essential for the observation of these processes.

[73] Although time-varying gravity observations from satellites can be used to derive bottom currents [*Wahr et al.*, 2002], it is currently not possible to infer the vertical velocity profile from satellite observations. The dynamic height signature of ocean circulation below the thermocline can be substantial [e.g., *Davis*, 2005]. To monitor this part of the global circulation, in situ observations such as those from the global Argo project [*Roemmich and Owens*, 2000] will continue to be indispensable.

[74] Global assimilation of both satellite and in situ data, as advocated by the GODAE project (http://www.bom.gov.au/bmrc/ocean/GODAE/), allow the combination of both satellite and in situ data into comprehensive analyses of the ocean circulation. For an assimilation system to give a reliable estimate, both observational and model errors will need to be known. Error estimates from model MDTs are generally lacking. A considerable effort has been made to set up model intercomparison projects [e.g., *Willebrand et al.*, 2001; *Griffies et al.*, 2000; *Griffies*, 2005], and to validate new model versions [e.g., *Chassignet et al.*, 2003; *Smith et al.*, 2000; *Maltrud and McClean*, 2005], but quantification of model error remains a delicate issue.

[75] In the present study, atmospheric forcing from different periods and data sources have been used to generate the mean sea level fields. As a consequence, low-frequency temporal variability in the sea level will affect the differences between the models. However, the differences between model solutions computed from the same period (for example, ORCA and MPI-OM both cover the last 50 years of the 20th century), suggest that the effects of differences between model parameterization and configuration are much larger than low-frequency temporal variations in sea level. Of course, it would be better to compute mean sea level over exactly the same simulation period, using exactly the same forcing fields, but this is beyond the scope of this study.

[76] It is not clear to what extent a ''mean dynamic topography'' really exists, as the ocean topography varies on all time scales. Also, it is unclear to what extent the ocean models have reached a steady state in the given simulation period. Simulation periods may not have been long enough for the models to reach a statistical equilibrium, specifically in the ACC, where the oceanic adjustment is relatively slow. Moreover, all models suffer from climate drift, and the effect of this drift on the MDT estimates has not been considered in the present study.

[77] Apart from the effects of difference in atmospheric forcing, averaging period, and (the lack of) internal equilibrium, there is a number of modeling aspects that will affect the model representation of dynamic topography. The effects of horizontal resolution [e.g., *Smith et al.*, 2000], the effects of bottom topography [e.g., *Marshall*, 1994] and vertical resolution [e.g., *Chassignet et al.*, 2003] on the simulation of mean sea level are known to be considerable. Moreover, the parameterization of mixing in the ocean models can contribute significantly to the differences between model and observational MDT estimates. Without performing a systematic model intercomparison, the present study identifies possible causes of differences between modeled and observed mean dynamic topography.

[78] To identify model errors and improve model formulation, combination of observations and models through data

assimilation can be instrumental. For example, methods have been developed to infer mixing coefficients from sea-level observations, although the potential of these methods is limited by the low sensitivity to mixing coefficients in regions of high eddy activity [*Vossepoel and van Leeuwen*, 2007]. The discrimination between the different error sources and eventually the improvement of ocean models is not possible without further observational evidence. To clarify the uncertainties listed above, a more accurate observational estimate of the mean dynamic topography is needed. If the GOCE gravity mission meets its objectives [*European Space Agency*, 1999], it is likely to contribute to such an estimate and shed light on the true uncertainties in the Earth's mean ocean dynamic topography.

[79] **Acknowledgments.** Peter Jan van Leeuwen (IMAU/Utrecht) contributed to this work through numerous discussions and comments on the interpretation of the results. This work also would not have been possible without the help and cooperation of a large number of people who willingly shared their data or model output. Marie-Helene Rio (CLS, Toulouse) provided the Rio05 MDT. Don Chambers (CSR, Austin) and Victor Zlotnicki (JPL, Pasadena) made their MDT available through the internet. Pascal LeGrand (Ifremer, Brest) and Ernst Schrama (DEOS, Delft) shared their MDT with me. I am grateful to Marc Naeije (DEOS, Delft) for his MDT and discussion of his results. The Maximenko-Niiler MDT was made available through internet by Nikolai Maximenko (IPRC, Honolulu) and Peter Niiler (SIO, La Jolla) (http://apdrc.soest.hawaii.edu/projects/DOT/). Keith Rodgers (LODYC, now at Princeton GFDL) provided the results of the ORCA model. Johann Jungclaus and Helmut Haak (MPI, Hamburg) shared their MPI-OM model results. Beverly de Cuevas and Andrew Coward (NOC, Southampton) provided the OCCAM data. Matthew Hecht and Mathew Maltrud (LANL, Los Alamos) made the POP sea level field available. Alan Wallcraft (NRL, Stennis) provided the HYCOM model output. Lucy Smedtstad and Charlie Barron (NRL, Stennis) provided the NCOM sea level field. The ECCO fields were made available through internet by the Estimating the Circulation and Climate of the Ocean (ECCO) consortium, funded by the National Oceanographic Partnership Program. Carl Wunsch and Patrick Heimbach (MIT, Cambridge) gave additional information on the ECCO model output. I am indebted to Nikolai Maximenko, Victor Zlotnicki, Don Chambers, Patrick Heimbach, Peter Niiler, and Alan Wallcraft for helpful suggestions to improve an earlier version of this manuscript. The comments of two anonymous reviewers are appreciated. Finally, discussions with Will de Ruijter (IMAU, Utrecht) and Radboud Koop (SRON, Utrecht) are greatly appreciated. This study is funded by the SRON-UU-DUT Framework Program "Space-based Observation of System Earth."

References

Auer, S. (1987), Five-year climatological survey of the Gulf Stream System and its associated rings, *J. Geophys. Res.*, *92*, 11,709–11,726.

Barron, C., A. Kara, P. Martin, R. Rhodes, and L. Smedstad (2006), Formulation, implementation and examination of vertical coordinate choices in the global Navy Coastal Ocean Model (NCOM), *Ocean Modell.*, *11*, 347–375.

Bingham, R., and K. Haines (2006), Mean dynamic topography: Intercomparisons and errors, *Philos. Trans. R. Soc., Ser. A*, *264*, 903–916.

Birol, F., J. M. Brankart, F. Castruccio, P. Brasseur, and J. Verron (2004), Impact of ocean mean dynamic topography on satellite data assimilation, *Mar. Geodesy*, *27*, 59–78.

Birol, F., J. M. Brankart, J. M. Lemoine, P. Brasseur, and J. Verron (2005), Assimilation of satellite altimetry referenced to the new GRACE geoid estimate, *Geophys. Res. Lett.*, *32*, L06601, doi:10.1029/2004GL021329.

Blanke, B., and P. Delecluse (1993), Variability of the tropical Atlantic ocean simulated by a general circulation model with two different mixed-layer physics, *J. Phys. Oceanogr.*, *23*, 1363–1387.

Bleck, R. (1998), Ocean modeling in isopycnic coordinates in *Ocean Modeling and Parameterization*, edited by E. P. Chassignet and J. Verron, pp. 423–448, Springer, New York.

Bleck, R., G. Halliwell, A. Wallcraft, S. Carroll, K. Kelly, and K. Rushing (2002), HYbrid Coordinate Ocean Model (HYCOM) user's manual, technical report, Rosenstiel School of Mar. and Atmos Sci., Miami, Fla. (Available at http://oceanmodeling.rsmas.miami.edu/hycom/doc/hycom-users-manual.pdf)

Blumberg, A., and G. Mellor (1987), A description of a three-dimensional coastal ocean circulation model, in *Three-Dimensional Coastal Ocean Models*, edited by N. Heaps, pp. 1–16, AGU, Washington, D. C.

Bryan, K. (1969), A numerical model for the study of the circulation of the World Ocean, *J. Comput. Phys.*, *4*, 347–376.

Canuto, V., A. Howard, P. Hogan, Y. Cheng, M. Dubovikov, and L. Montenegro (2004), Modelling ocean deep convection, *Ocean Modell.*, *7*, 75–95.

Carnes, M., D. Fox, R. Rhodes, and O. Smedstad (1996), Data assimilation in a North Pacific Ocean monitoring and prediction system, in *Modern Approaches to Data Assimilation in Ocean Modeling*, vol. 61, edited by P. Malanotte-Rizzoli, pp. 319–345, Elsevier, New York.

Chambers, D., and V. Zlotnicki (2004), GRACE products for oceanography, in paper presented at Ocean Surface Topography Science Team Meeting, Cent. Natl. 0d'Etudes Spatiales, St Petersburg, Fla.

Chassignet, E. P., L. T. Smith, R. Halliwell, and G. R. Bleck (2003), North Atlantic simulations with the Hybrid Coordinate Ocean Model (HYCOM): Impact of the vertical coordinate choice, reference pressure, and thermobaricity, *J. Phys. Oceanogr.*, *33*, 2504–2526.

Chassignet, E. P., et al. (2006), Generalized vertical coordinates for eddy-resolving global and coastal ocean forecasts, *Oceanography*, *19*, 20–31.

Cheney, R., and J. Marsh (1981), Seasat altimeter observations of dynamic topography in the Gulf-Stream region, *J. Geophys. Res.*, *86*, 473–483.

Conkright, M. E., et al. (2002), *World Ocean Database 2001*, vol. 1, *Introduction, NOAA Atlas NESDIS 42*, 160 pp., Natl. Oceanic and Atmos. Admin., Silver Spring, Md.

Coward, A., de B. A. Cuevas (2005), The OCCAM 66 level model: Physics, initial conditions and external forcing, *SOC Rep. 99*, Natl Oceanogr. Cent., Southampton, U. K. (Available at http://www.noc.soton.ac.uk/JRD/OCCAM/OCCAM-p25k66-run202.pdf)

Cox, M. D. (1984), A primitive, 3-dimensional model of the ocean, *GFDL Ocean Group Tech. Rep. 1*, Geophys. Fluid Dyn. Lab./NOAA, Princeton Univ., Princeton, N. J.

Cox, M. (1997), Isopycnal diffusion in a z-coordinate ocean model, *Ocean Modell.*, *74*, 1–9.

Davis, R. E. (2005), Intermediate-depth circulation of the Indian and South Pacific Oceans measured by autonomous floats, *J. Phys. Oceanogr.*, *35*, 683–707.

Denker, H., and R. H. Rapp (1990), Geodetic and oceanographic results from the analysis of 1 year of Geosat data, *J. Geophys. Res.*, *95*, 13,151–13,168.

Dijkstra, H., and W. P. M. de Ruijter (2001), On the physics of the Agulhas Current: Steady retroflection regimes, *J. Phys. Oceanogr.*, *31*, 2971–2985.

Dukowicz, J., and R. Smith (1994), Implicit free-surface method for the Bryan-Cox-Semtner ocean model, *J. Geophys. Res.*, *99*, 7991–8014.

Engelis, T., and P. Knudsen (1989), Orbit improvement and determination of the ocean geoid and topography from 17 days of Seasat data, *Manuscr. Geod.*, *14*, 193–201.

European Space Agency (1999), The four candidate Earth Explorer Core Missions: Gravity Field and Steady-State Ocean Circulation Explorer, *Eur. Space Agency Spec. Publ., ESA Sp-1233*, 217 pp.

Forge, G., and C. Wunsch (2007), Global hydrographic variability and the data weights in oceanic state estimates, *J. Phys. Oceanogr*, in press.

Fox, D., W. Teague, C. Barron, M. Games, and C. Lee (2002), The Modular Ocean Data Analysis System (MODAS), *J. Atmos. Oceanic Technol.*, *19*, 240–252.

Fu, L.-L. (2006), Pathways of eddies in the South Atlantic revealed from satellite altimeter observations, *Geophys. Res. Lett.*, *33*, L14610, doi:10.1029/2006GL026245.

Gent, P. R., and J. C. McWilliams (1990), Isopycnal mixing in ocean circulation models, *J. Phys. Oceanogr.*, *20*, 150–156.

Gent, P. R., J. Willebrand, T. McDougall, and J. C. McWilliams (1995), Parameterizing eddy induced tracer transports in ocean circulation models, *J. Phys. Oceanogr.*, *25*, 463–474.

Gibson, J., P. Kallberg, S. Uppala, A. Hernandez, A. Nomura, and E. Serrano (1997), ECMWF Re-analysis. 1. ERA description, technical report, Eur. Cent. for Medium-Range Weather Forecasts, Reading, U. K.

Giering, R., and T. Kaminski (1998), Recipes for adjoint code construction, *Trans. Math. Software*, *24*, 437–474.

Gille, S. (2003), Float observations of the southern ocean: Part 1, estimating mean fields, bottom velocities, and topographic steering, *J. Phys. Oceanogr.*, *33*, 1167–1181.

Gordon, A. L., and E. M. Molinelli (1986), *Southern Ocean Atlas: Thermohaline-Chemical Distributions and the Atlas Data Set*, 11 pp. +233 plates, Columbia Univ. Press, New York.

Gordon, A. L., E. Molinelli, and T. Baker (1978), Large-scale relative dynamic topography of the Southern Ocean, *J. Geophys. Res.*, *83*, 3023–3032.

Gouretski, V. V., and K. Jancke (2001), Systematic errors as the cause for an apparent deep water property variability: Global analysis of the WOCE and historical hydrographic data, *Prog. Oceanogr.*, *48*, 337–402.

Gouretski, V. V., and K. P. Koltermann (2004), WOCE global hydrographic climatology: A technical report, *Ber. Bundes. Schiff. Hydrogr.*, vol. 35, Bundesamt für Schifffahrt und Hydrogr., Hamburg, Germany.

Griffies, S. (1998), The Gent-McWilliams skew flux, *J. Phys. Oceanogr.*, *28*, 831–841.

Griffies, S. (2005), Some ocean model fundamentals in *Ocean Weather Forecasting: An Integrated View of Oceanography*, edited by E. P. Chassignet and J. Verron, pp. 19–74, Springer, New York.

Griffies, S., C. Böning, F. O. Bryan, E. P. Chassignet, R. Gerdes, H. Hasumi, A. Hirst, A.-M. Treguier, and D. Webb (2000), Developments in ocean climate modelling, *Ocean Modell.*, *2*, 123–192.

Halliwell, G. (1998), Simulation of North Atlantic decadal/multi-decadal winter SST anomalies driven by basin-scale atmospheric circulation anomalies, *J. Phys. Oceanogr.*, *28*, 5–21.

Halliwell, G., R. Bleck, E. Chassignet, and L. Smith (1999), Mixed layer model validation in Atlantic Ocean simulations using the HYbrid Coordinate Ocean Model (HYCOM), *Eos Trans. AGU*, *80*(49), Ocean Sci. Meet. Suppl., OS304.

Hernandez, F., and P. Schaeffer (2001), The CLS Mean Sea Surface: A validation with the GSFC00.1 surface, Tech. Rep. *AVI-NT-011-5242-CLS*, Collecte Localisation Satell., Ramonville, France.

Hernandez, F., et al. (2001), Surface Moyenne Oceanique: Support Scientifique á la mission altimétrique Jason-1, et á une mission micro-satellite altimétrique, *Contrat SSALTO 2945-Lot2-A.1, Rapp. Final CLS/DOS/NT/00.341*, Collecte Localisation Satell., Ramonville, France.

Hughes, C. (2005), Nonlinear vorticity balance of the Antarctic Circumpolar Current, *J. Geophys. Res.*, *110*, C11008, doi:10.1029/2004JC002753.

Jayne, S. (2006), Circulation of the North Atlantic Ocean from altimetry and the Gravity Recovery and Climate Experiment geoid, *J. Geophys. Res.*, *111*, C03005, doi:10.1029/2005JC003128.

Kalnay, E., et al. (1996), The NCEP/NCAR 40-year reanalysis project, *Bull. Am. Meteorol. Soc.*, *77*, 437–471.

Kara, A. B., C. Barron, P. J. Martin, L. F. Smedstad, and R. C. Rhodes (2006), Validation of interannual simulations from the 1/8° global Navy Coastal Ocean Model (NCOM), *Ocean Modell.*, *11*, 376–398.

Large, W. G., and S. Pond (1981), Open ocean momentum flux measurements in moderate to strong winds, *J. Phys. Oceanogr.*, *11*, 324–336.

Large, W. G., J. C. McWilliams, and S. C. Doney (1994), Oceanic vertical mixing: A review and a model with a nonlocal boundary layer parameterization, *Rev. Geophys.*, *32*, 363–403.

Lazar, A., G. Madec, and P. Delecluse (1999), The deep interior downwelling, the Veronis effect, and mesoscale tracer transport parametrizations in an OGCM, *J. Phys. Oceanogr.*, *29*, 2945–2961.

Lee, M.-M., A. Coward, and A. Nurser (2002), Spurious diapycnal mixing of the deep waters in an eddy-permitting global ocean model, *J. Phys. Oceanogr.*, *32*, 1522–1535.

LeGrand, P. (2001), Impact of the Gravity Field and Steady-State Ocean Circulation Explorer (GOCE) mission on ocean circulation estimates: Volume fluxes in a climatological inverse model of the Atlantic, *J. Geophys. Res.*, *106*, 19,597–19,610.

LeGrand, P., H. Mercier, and T. Reynaud (1998), Combining T/P altimetric data with hydrographic data to estimate the mean dynamic topography of the North Atlantic and improve the geoid, *Ann. Geophys.*, *16*, 638–650.

LeGrand, P., E. Schrama, and J. Tournadre (2003), An inverse estimate of the dynamic topography of the ocean, *Geophys. Res. Lett.*, *30*(2), 1062, doi:10.1029/2002GL014917.

Legutke, S., and E. Maier-Reimer (2002), The impact of downslope water-transport parameterization in a global ocean general circulation model, *Clim. Dyn.*, *18*, 611–623.

Lemoine, F., N. Pavlis, S. Kenyon, R. Rapp, E. Pavlis, and B. Chao (1998), New high-resolution model developed for Earth's gravitational field, *Eos Trans. AGU*, *79*, 117–118.

Levitus, S., T. P. Boyer, M. E. Conkright, T. O'Brien, J. Antonov, C. Stephens, L. Stathoplos, D. Johnson, and R. Gelfeld (1998), *World Ocean Database 1998, vol. 1 Introduction, NOAA Atlas NESDIS 18*, 346 pp., Natl. Oceanic and Atmos. Admin., Silver Spring, Md.

Losch, M., and J. Schröter (2004), Estimating the circulation from hydrography and satellite altimetry in the Southern Ocean: Limitations imposed by the current geoid models, *Deep Sea Res., Part 1*, *51*, 1131–1143.

Losch, M., B. Sloyan, J. Schröter, and N. Sneeuw (2002), Box inverse models, altimetry and the geoid: Problems with the omission error, *J. Geophys. Res.*, *107*(C7), 3078, doi:10.1029/2001JC000855.

Lu, Y., K. Ueyoshi, A. Köhl, E. Remy, K. Lorbacher, and D. Stammer (2002), Input data sets for the ECCO global 1° WOCE synthesis, report, Scripps Inst. of Oceanogr., La Jolla, Calif.

Madec, G., P. Delecluse, M. Imbard, and C. Levy (1998), OPA 8.1 Ocean General Circulation Model reference manual, *Note Pole Model. 11*, Inst. Pierre Simon Laplace, Paris.

Maltrud, M., and J. L. McClean (2005), An eddy resolving global 1/10° ocean simulation, *Ocean Modell.*, *8*, 31–54.

Marshall, D. (1994), Influence of topography on the large-scale ocean circulation, *J. Phys. Oceanogr.*, *7*, 1622–1635.

Marshall, J., A. Adcroft, C. Hill, L. Perelman, and C. Heisey (1997), A finite volume, incompressible Navier-Stokes model for studies of the ocean on parallel computers, *J. Geophys. Res.*, *102*, 5753–5766.

Marsland, S., H. Haak, J. Jungclaus, M. Latif, and F. Röske (2003), The Max-Planck-Institute global ocean/sea ice model with orthogonal curvilinear coordinates, *Ocean Modell.*, *5*, 91–127.

Martin, P. (2002), Description of the Navy Coastal Ocean Model Version 1.0., *Tech. Rep. NRL/FR/7322/00/9962*, Naval Res. Lab., Stennis Space Center, Miss.

Maximenko, N., and P. P. Niiler (2004), Hybrid decade-mean global sea level with mesoscale resolution, in *Recent Advances in Marine Science and Technology*, edited by N. Saxena, pp. 55–59, PACON Int, Honolulu, Hawaii.

Mercier, H., M. Ollitrault, and P.-Y. L. Traon (1993), An inverse model of the North Atlantic general circulation using Lagrangian float data, *J. Phys. Oceanogr.*, *23*, 698–715.

Nerem, R. S., B. D. Tapley, and C. K. Shum (1990), Determination of the ocean circualtion using Geosat altimetry, *J. Geophys. Res.*, *95*, 3163–3179.

Niiler, P. (2001), The World Ocean surface circulation in *Ocean Circulation and Climate-Observing and Modeling the Global Ocean*, edited by J. Church, G. Siedler, and J. Gould, pp. 193–204, Elsevier, New York.

Niiler, P., N. Maximenko, and J. McWilliams (2003), Dynamically balanced absolute sea level of the global ocean derived from near-surface velocity observations, *Geophys. Res. Lett.*, *30*(22), 2164, doi:10.1029/2003GL018628.

Olbers, D., V. Gouretski, G. Sei, and J. Schroeter (1992), *Hydrographic Atlas of the Southern Ocean*, xvii pp. +82 plates, Alfred-Wegener Inst., Bremerhaven, Germany.

Pacanowski, R. C., and S. M. Griffies (1998), MOM3.0 manual, technical report, Geophys. Fluid Dyn. Lab., NOAA, Princeton, N. J.

Ponte, R. M., C. Wunsch, and D. Stammer (2007), Spatial mapping of time-variable errors in Jason-1 and TOPEX/Poseidon sea surface height measurements, *J. Atmos. Ocean. Technol.*, in press.

Ralph, E. A., and P. P. Niiler (1999), Wind-driven currents in the tropical Pacific, *J. Phys. Oceanogr.*, *29*, 2121–2129.

Rapp, R. H., C. Zhang, and Y. Yi (1996), Analysis of dynamic ocean topography using TOPEX data and orthonormal functions, *J. Geophys. Res.*, *101*, 22,583–22,598.

Reid, J. L. (1997), On the total geostrophic circulation of the Pacific Ocean: Flow patterns, tracers, and transports, *Prog. Oceanogr.*, *39*, 263–352.

Reigber, C., R. Schmidt, F. Flechtner, R. Koenig, U. Meyer, K. H. Neumayer, P. Schwintzer, and S. Y. Zhu (2005), An Earth gravity field model complete to degree and order 150 from GRACE: EIGEN-GRACE02S, *J. Geodyn.*, *39*, 1–10.

Reynolds, R. W., N. A. Rayner, T. M. Smith, D. C. Stokes, and W. Wang (2002), An improved in situ and satellite SST analysis for climate, *J. Clim.*, *715*, 1609–1625.

Rio, M.-H., and F. Hernandez (2004), A mean dynamic topography computed over the World Ocean from altimetry in situ measurements and a geoid model, *J. Geophys. Res.*, *109*, C12032, doi:10.1029/2003JC002226.

Rio, M.-H., P. Schaeffer, F. Hernandez, and J.-M. Lemoine (2005), The estimation of the ocean Mean Dynamic Topography through the combination of altimetric data, in-situ measurements and GRACE geoid: From global to regional studies, paper presented at GOCINA Workshop, GOCINA Project, Eur. Union, Luxembourg.

Roemmich, D., and W. Owens (2000), The Argo Project: Global ocean observations for understanding and prediction of climate variability, *Oceanography*, *13*, 45–50.

Roullet, G., and G. Madec (2000), Salt conservation, free surface and varying volume: A new formulation for ocean GCMs, *J. Geophys. Res.*, *105*, 23,927–23,942.

Schröter, J., M. Losch, and B. Sloyan (2002), Impact of the Gravity Field and Steady-State Ocean Circulation Explorer (GOCE) mission on ocean circulation estimates: 2. Volume and heat fluxes across hydrographic sections of unequally spaced stations, *J. Geophys. Res.*, *107*(C2), 3012, doi:10.1029/2000JC000647.

Semtner, A. J. (1974), An oceanic general circulation model with bottom topography, technical report, Dep. of Meteorol. Technol., Univ. of Calif., Los Angeles.

Smedstad, O. M., H. E. Hurlburt, E. J. Metzger, R. C. Rhodes, J. F. Shriver, A. J. Wallcraft, and A. B. Kara (2003), An operational eddy

resolving 1/16 global ocean nowcast/forecast system, *J. Mar. Syst.*, *40-41*, 341–361.

Smith, R., M. Maltrud, F. Bryan, and M. Hecht (2000), Numerical simulation of the North Atlantic Ocean at 1/10, *J. Phys. Oceanogr.*, *30*, 1532–1561.

Stammer, D. C. W. (1994), Preminary assessment of the accuracy and precision of TOPEX/Poseidon altimeter data with respect to the large-scale ocean circulation, *J. Geophys. Res.*, *99*, 24,584–24,604.

Stammer, D., R. Tokmakian, A. Semtner, and C. Wunsch (1996), How well does a 1/4° global circulation model simulate large-scale oceanic observations?, *J. Geophys. Res.*, *101*, 25,779–25,812.

Stammer, D., C. Wunsch, R. Giering, C. Eckert, P. Heimbach, J. Marotzke, A. Adcroft, C. N. Hill, and J. Marshall (2002), Global ocean circulation during 1992–1997, estimated from ocean observations and a general circulation model, *J. Geophys. Res.*, *107*(C9), 3118, doi:10.1029/2001JC000888.

Stammer, D., C. Wunsch, R. Giering, C. Eckert, P. Heimbach, J. Marotzke, A. Adcroft, C. N. Hill, and J. Marshall (2003), Volume, heat, and freshwater transports of the global ocean circulation 1993–2000, estimated from a general circulation model constrained by World Ocean Circulation Experiment (WOCE) data, *J. Geophys. Res.*, *108*(C1), 3007, doi:10.1029/2001JC001115.

Sverdrup, H., M. Johnson, and R. Fleming (1942), *The Oceans: Their Physics, Chemistry, and General Biology*, Prentice-Hall, Upper Saddle River, N. J.

Tapley, B., D. Chambers, S. Bettadpur, and J. Ries (2003), Large scale ocean circulation from the GRACE GGM01 geoid, *Geophys. Res. Lett.*, *30*(22), 2163, doi:10.1029/2003GL018622.

Thorpe, S., D. P. Stevens, and K. J. Heywood (2005), Comparison of two time-variant forced eddy-permitting global ocean circulation models with hydrography of the Scotia Sea, *Ocean Modell.*, *9*, 105–132.

Vossepoel, F. C., and P. J. van Leeuwen (2007), Parameter estimation using a particle method: Inferring mixing coefficients from sea-level observations, *Mon. Weather Rev.*, *135*, 1006–1020.

Wagner, C., and O. L. Colombo (1979), Gravitational spectra from direct measurements, *J. Geophys. Res.*, *84*, 4699–4712.

Wahr, J. M., S. R. Jayne, and F. O. Bryan (2002), A method of inferring changes in deep ocean currents from satellite measurements of time-variable gravity, *J. Geophys. Res.*, *107*(C12), 3218, doi:10.1029/2001JC001274.

Wallcraft, A., A. Kara, H. Hurlburt, and P. Rochford (2003), The NRL Layered Global Ocean model (NLOM) with an embedded mixed layer sub-model: Formulation and tuning, *J. Atmos. Oceanic Technol.*, *20*, 1601–1615.

Wang, Y. (2001), GSFC00 mean sea surface, gravity anomaly, and vertical gravity gradient from satellite altimeter data, *J. Geophys Res.*, *106*, 31,167–31,174.

Watts, D. R., K. L. Tracey, J. M. Bane, and T. J. Shay (1995), Gulf stream path and thermocline structure near 74°w and 68°w, *J. Geophys. Res.*, *100*, 18,291–18,312.

Webb, D. J., de B. A. Cuevas, and A. C. Coward (1998), The first main run of the OCCAM global ocean model, internal document, Southampton Oceanogr. Centre, Southampton, U. K.

Willebrand, J., C. B. B. Barnier, C. Dieterich, P. D. Killworth, C. L. Provost, Y. Jia, J.-M. Molines, and A. L. New (2001), Circulation characteristics in three eddy-permitting models of the North Atlantic, *Prog. Oceanogr.*, *48*, 123–161.

Wunsch, C. (1978), The North Atlantic general circulation west of 50°W determined by inverse methods, *Rev. Geophys.*, *16*, 583–620.

Wunsch, C. (1996), *The Ocean Circulation Inverse Problem*, 442 pp., Cambridge Univ. Press, New York.

Wunsch, C., and P. Heimbach (2006), Estimated decadal changes in the North Atlantic Meridional Overturning Circulation and heat flux 1993–2004, *J. Phys. Oceanogr.*, *36*, 2012–2024.

Wunsch, C., and P. Heimbach (2007), Practical global oceanic state estimation, *Physica D*, doi:10.1016/j.physd.2006.09.040, in press.

Zlotnicki, V. (1984), On the accuracy of gravimetric geoids and the recovery of oceanographic signals from altimetry, *Mar. Geod.*, *8*, 129–157.

F. C. Vossepoel, Shell International Exploration and Production B.V., Kesslerpark 1, NL-2288 Rijswijk, Netherlands. (Femke.Vossepoel@shell.com)